DISSERTATIONES
TECHNOLOGIAE
UNIVERSITATIS
TARTUENSIS
49

INGA PÕLDSALU

Soft actuators with ink-jet printed electrodes

DISSERTATIONES TECHNOLOGIAE UNIVERSITATIS TARTUENSIS
49

INGA PÕLDSALU

Soft actuators with ink-jet printed electrodes

UNIVERSITY OF TARTU
Press

Institute of Technology, Faculty of Science and Technology, University of Tartu, Estonia

This dissertation was accepted for the commencement of the degree of Doctor of Philosophy in Physical Engineering on October 15th, 2018 by the Council of the Institute of Technology, Faculty of Science and Technology, University of Tartu, Estonia.

Supervisors: Dr. Anna-Liisa Peikolainen,
Institute of Technology, University of Tartu, Estonia

Dr. Rudolf Benedikt Kiefer,
Faculty of Applied Sciences, Ton Duc Thang University,
HCMC, Vietnam

Opponent: Dr. Christian Bergaud,
French National Center for Scientific Research, France

Commencement: Auditorium 121, Nooruse 1, Tartu, Estonia,
at 14:15 on November 30th, 2018

Publication of this dissertation is granted by the Institute of Technology, Faculty of Science and Technology, University of Tartu

ISSN 2228-0855
ISBN 978-9949-77-903-1 (print)
ISBN 978-9949-77-904-8 (pdf)

University of Tartu Press
www.tyk.ee

TABLE OF CONTENTS

LIST OF ORIGINAL PUBLICATIONS 6
Author's contribution 6
Other publications in related field 6
ABBREVIATIONS 8
1. INTRODUCTION 9
2. MOTIVATION AND SCOPE 10
3. IONIC ELECTROACTIVE POLYMER ACTUATORS 11
3.1 Applications in the field 11
3.2 Conducting polymer based ionic electromechanical actuators 12
3.2.1 Actuation mechanism 12
3.2.2 Architecture of the actuator 15
4 INK-JET PRINTING TECHNOLOGY FOR IEAP FABRICATION 17
4.1 Inkjet printing technology 17
4.2 Suspensions of conducting polymers 19
4.3 Strategy of printing and actuator preparation 20
4.4 Characterisation of the actuators 22
4.4.1 Mechanical properties 22
4.4.2 Electromechanical and electro-chemo-mechanical properties 22
5. RESULTS AND DISCUSSION 27
5.1 Control over electrical, mechanical and electromechanical properties of the actuators 27
5.2 Electromechanical properties 29
5.3 Influence of conducting polymer-carbon-composite electrodes on actuator properties 32
5.4 Miniaturisation 35
6. CONCLUSIONS 39
7. SUMMARY IN ESTONIAN 40
REFERENCES 42
ACKNOWLEDGEMENTS 46
PUBLICATIONS 47
CURRICULUM VITAE 77
ELULOOKIRJELDUS 80

LIST OF ORIGINAL PUBLICATIONS

I. Põldsalu, I., Harjo, M., Tamm, T., Uibu, M., Peikolainen, A.-L. & Kiefer, R. Inkjet-printed hybrid conducting polymer-activated carbon aerogel linear actuators driven in an organic electrolyte. *Sensors Actuators B Chem.* **250,** 44–51 (2017).

II. Põldsalu, I., Johanson, U., Tamm, T., Punning, A., Greco, F., Peikolainen, A.-L., Kiefer, R., Aabloo, A. Mechanical and electro-mechanical properties of EAP actuators with inkjet printed electrodes. *Synthetic Metals,* **246,** 122-127 (2018).

III. Põldsalu, I., Rohtlaid, K., Nguyen, T. M. G., Plesse, C., Vidal, F., Khorram, M. S., Peikolainen, A.-L., Tamm, T. & Kiefer, R. Thin ink-jet printed trilayer actuators composed of PEDOT:PSS on interpenetrating polymer networks. *Sensors Actuators B Chem.* **258,** 1072–1079 (2018).

Author's contribution

In publication I, the author was involved in planning the experiments, data analysis and writing the manuscript. In the experimental part, the author was responsible for fabrication of conducting polymer and conducting polymer-carbon-composite actuators and elaboration of the fabrication methodology.

In publication II, the author conducted all the experimental work from fabrication to characterisation of the actuators. Through being engaged in planning experiments, data analysis and interpretation, she was the main writer and the corresponding author of the manuscript.

In publication III, the author conducted micro-printing of the electrode materials and prepared the micro-actuators, carried out the electromechanical characterisation in bending mode and was involved in data analysis. The author was one of the main contributors to writing the manuscript.

Other publications in related field

- Nakshatharan, S. S., Vunder, V., Põldsalu, I., Johanson, U., Punning, A. & Aabloo, A. Modelling and Control of Ionic Electroactive Polymer Actuators under Varying Humidity Conditions. *Actuators* **7,** 7 (2018).
- Põldsalu, I., Mändmaa, S.-E., Peikolainen, A.-L., Kesküla, A. & Aabloo, A. Fabrication of ion-conducting carbon polymer composite electrodes by spin coating. in *Proc. SPIE 9430, Electroactive Polymer Actuators and Devices (EAPAD)* **9430,** 943019 (2015).

- Kaasik, F., Must, I., Baranova, I., Põldsalu, I., Lust, E., Johanson, U., Punning, A. & Aabloo, A. Scalable fabrication of ionic and capacitive laminate actuators for soft robotics. *Sensors Actuators B Chem.* **246,** 154–163 (2017).
- Must, I., Kaasik, F., Põldsalu, I., Mihkels, L., Johanson, U., Punning, A. & Aabloo, A. Ionic and capacitive artificial muscle for biomimetic soft robotics. *Adv. Eng. Mater.* **17,** 84–94 (2015).
- Punning, A., Kim, K. J., Palmre, V., Vidal, F., Plesse, C., Festin, N., Maziz, A., Askaka, K., Sugino, T., Alici, G., Spinks, G., Wallace, G., Must, I., Põldsalu, I., Vunder, V., Temmer, R., Kruusamäe, K., Torop, J., Kaasik, F., Rinne, P., Johanson, U., Peikolainen, A.-L., Tamm, T., Aabloo, A. Ionic electroactive polymer artificial muscles in space applications. *Sci. Rep.* **4,** 1–6 (2014).
- Punning, A., Must, I., Põldsalu, I., Vunder, V., Temmer, R., Kruusamäe, K., Kaasik, F., Torop, J., Rinne, P., Lulla, T., Johanson, U., Tamm, T. & Aabloo, A. Lifetime measurements of ionic electroactive polymer actuators. *J. Intell. Mater. Syst. Struct.* **25,** 2267–2275 (2014).
- Must, I., Vunder, V., Kaasik, F., Põldsalu, I., Johanson, U., Punning, A. & Aabloo, A. Ionic liquid-based actuators working in air: The effect of ambient humidity. *Sensors Actuators B Chem.* **202,** 114–122 (2014).
- Vunder, V., Itik, M., Põldsalu, I., Punning, A. & Aabloo, A. Inversion-based control of ionic polymer-metal composite actuators with nanoporous carbon-based electrodes. *Smart Mater. Struct.* **23,** (2014).
- Must, I., Kaasik, F., Põldsalu, I., Mihkels, L., Johanson, U., Punning, A. & Aabloo, A. Pulse-width-modulated charging of ionic and capacitive actuators. in *IEEE/ASME International Conference on Advanced Intelligent Mechatronics, AIM* 1446–1451 (2014).
- Must, Indrek; Anton, Mart; Viidalepp, Erki; Põldsalu, Inga; Punning, Andres; Aabloo, Alvo (2013).
- Must, I., Anton, M., Viidalepp, E., Põldsalu, I., Punning, A. & Aabloo, A. Mechanoelectrical impedance of a carbide-derived carbon-based laminate motion sensor at large bending deflections. *Smart Mater. Struct.* **22,** 104015 (2013).
- Must, I., Johanson, U., Kaasik, F., Poldsalu, I., Punning, A. & Aabloo, A. An ionic liquid-based actuator as a humidity sensor. *2013 IEEE/ASME Int. Conf. Adv. Intell. Mechatronics Mechatronics Hum. Wellbeing, AIM 2013* 1498–1503 (2013).
- Must, I., Kaasik, F., Põldsalu, I., Johanson, U., Punning, A. & Aabloo, A. A carbide-derived carbon laminate used as a mechanoelectrical sensor. *Carbon N. Y.* **50,** 535–541 (2012).

ABBREVIATIONS

[EMIm][TfO]	1-ethyl-3-methylimidazolium trifluoromethanesulfonate
[EMIm][TFSI]	1-ethyl-3-methylimidazolium bis(trifluoromethylsulfonyl)imide
ACA	activated carbon aerogel
CDC	Carbide-derived carbon
CP	conducting polymer
CV	cyclic voltammetry
DOD	drop-on-demand
EAP	electro-active polymer
EC	electrochemical
ECMD	electro-chemo-mechanical deformation
EDL	electric double layer
EDX	energy dispersive X-ray spectrometry
E_{EM}	equivalent electromechanical elastic modulus
E_M	equivalent mechanical elastic modulus
IEAP	ionic electromechanically active polymer
IL	ionic liquid
IPMC	ionic polymer-metal composite
IPN	interpenetrating polymer network
MEMS	microelectromechanical systems
NBR	nitrile butadiene rubber
OLED	organic light emitting diode
PC	propylene carbonate
PEDOT:PSS	poly(3,4-ethylenedioxythiophene) polystyrene sulfonate
PEO	poly(ethylene oxide)
PPy	polypyrrole
PVdF	poly(vinylidene fluoride)
Py	pyrrole
SEM	scanning electron microscopy

1. INTRODUCTION

Actuators imitating natural muscles (artificial muscles) are essential in robotics, medicine, biotechnology and in many fields where properties, such as longitudinal movement, volumetric effect, miniaturisation, silent operation and biocompatibility are required.

Soft ionic electromechanical actuators are attractive for the gentle manipulation of objects. Ionic type electromechanical actuators are single- or multilayered films that mechanically respond to electrical stimuli. Due to their attractive low operating voltage, large strain response, large contraction force and quick response, they have been studied since they were proposed as actuator materials by Baughman et al. [1] to improve their actuation performance and develop fabrication methodologies with high reproducibility.

One of the exceptional features of ionic electromechanically active polymer (IEAP) composites compared to electromechanical actuators driven by an electric rotary motor is their miniaturisability by reducing the film dimensions by cutting, and this opens up applications in micro-scale, such as the micromanipulation of living cells in bio-analytical nanosystems; in lab- on-chips as microvalves, microswitches, micropumps or microshutters; cantilever light modulators in micro-optical instrumentation; artificial muscles for microrobotics and more [2]. As such, IEAPs can operate as mechano-electrical sensors, broadening the field of applications even further. The manufacturing technology must be carefully chosen so that micro-actuators could be produced by utilising industrial machinery for large scale fabrication. The current work investigates the applicability of printing technology for the fabrication of ionic electromechanical systems of tri-layered IEAP composites based on conducting polymers. To date, the techniques of applying ionic electromechanically active layers of the film have mainly involved casting, spray painting, spin coating, and chemical (e.g. vapor phase polymerisation) and electrochemical polymerisation. These techniques are quite unsustainable regarding the use of material: the electroactive material is applied across the whole substrate, but thickness variations across one sample often causes significant amounts of waste and difficulties with reproducibility in fabrication. Laser cutting has been demonstrated in obtaining miniature actuator films, but the main drawbacks include the excessive use of materials and the risk of melting the film, leading to malfunctioning of the actuator. Drop-on-demand (DOD) printing can solve these problems and it presents the option to design and fabricate complex and intricate patterns. This work is dedicated to the fabrication of soft actuators with inkjet-printed electrodes to show that inkjet printing is a compatible technology for the fabrication of ionic electromechanical systems.

2. MOTIVATION AND SCOPE

The research focus in this work was to transfer actuator fabrication into micro-scale using industrially compatible ink-jet printing technology. The main goal was both to implement established technologies used for large scale production, thereby enhancing the reproducibility compared to manual fabrication methods, and to develop microactuators with controlled behavior using inkjet printing. The following hypotheses were addressed:

- Ionic electromechanical systems can be fabricated using ink-jet printing technology; carbon-polymer composites can be printed as an electrode for actuators.

  Publication I studies conducting polymer actuators and conducting polymer-carbon-composite actuators. It was shown for the first time that inkjet printing can be equally applied for the fabrication of conducting polymer and conducting polymer-carbon-composite actuators. The majority of three-layer actuators are studied in bending mode, where linear actuation and ion-transport properties were studied. Conducting polymer-based actuators were more suitable for applications requiring higher strain and conducting polymer-carbon-composite based actuators for applications requiring higher force.
- It is possible to tailor the properties of the actuator with layer-wise growth of the electrodes.

  Publication II studies the possibilities of tailoring the mechanical, electro-mechanical and chemical properties of the bending actuators solely by varying the electrode thickness. It is achieved with the controlled growth of ink-jet printed layers of conducting polymer-based electrodes on commercial poly(vinylidene fluoride) (PVdF) membranes. The same effects were investigated in the case of conducting polymer-carbon-composite IEAPs. These bending type actuators were described by measuring strain, blocking force and capacitance.
- Microactuators can be fabricated using ink-jet printing and spin coating technologies and they can be used in linear actuation mode as well as in bending actuation mode.

  Publication III focuses on the fabrication of very thin actuators by using industrially applicable fabrication for printing conducting polymer electrodes on spin coated membranes. The total thickness of the actuator was ~10 μm as opposed to ~100 μm in the previous publications.

3. IONIC ELECTROACTIVE POLYMER ACTUATORS

3.1 Applications in the field

In many small devices there is a need for smaller actuators, where conventional electromagnetic rotary motors, hydraulic or pneumatic systems are too big, heavy, noisy, complex or otherwise unsuitable. Soft microactuators are required where applications require gentle operation such as the micromanipulation of biological samples [3], micromechanical stimulation of single cells [4], operation of valves in microfluidics [5]. Microactuators have been fabricated using different physical principles [6], including thermal expansion [7], magnetism [8] and electrostatic forces [9] (Figure 1), but they utilise stiff materials and can be harmful for manipulating fragile objects. Another class of actuators is electroactive polymers (EAPs), which respond to electrical stimuli by changing their volume, shape, stiffness or stress. The elasticity and processability of EAPs make them attractive as actuators. In addition, they have advantages over conventional actuators, as they are typically simple and flexible in their design, have simultaneous sensing ability [10,11] and silent operation, and are versatile for various applications.

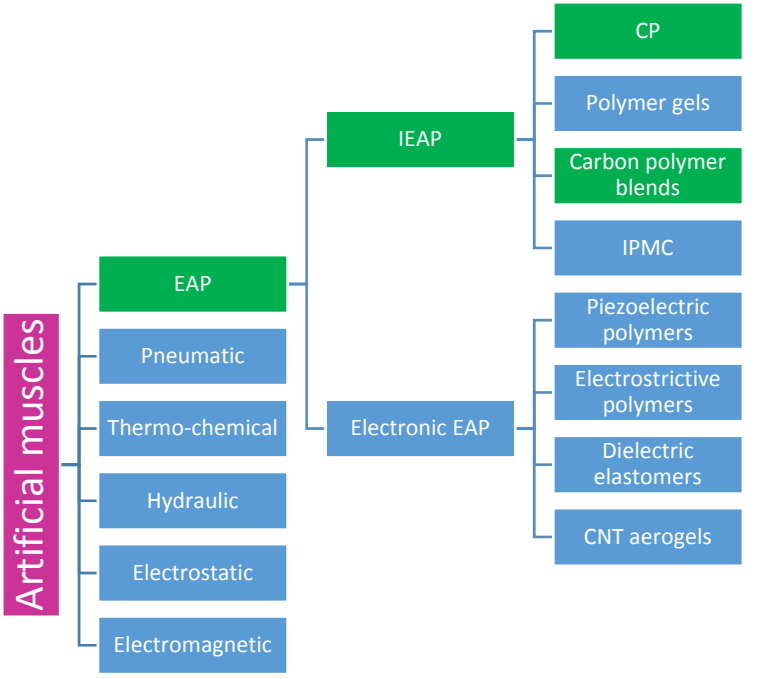

Figure 1. Classification of artificial muscles [12]

EAP actuators can be divided into two groups: dielectric and ionic EAP actuators (Figure 1). In dielectric EAPs, the actuation is caused by electrostatic forces. They have high stress and energy density, are fast and efficient and do not need electrolytes. However, high driving voltage (kV range) by signal polarity or signal intensity are its significant disadvantages. In ionic EAPs, actuation is caused by the electrically driven motion of ions or its solvent shells. Based on electroactive material, IEAPs can be divided further into conducting polymer (CP) based IEAPs, ionic polymer-metal composites (IPMC), polymer gels and carbon-based ionic IEAPs [12].

3.2 Conducting polymer based ionic electromechanical actuators

Microactuators based on reduction-oxidation reaction of CPs have many attractive features such as being electrically controlled, having low activation voltage (0.5… 5 V) [13], large strain (up to 20%)[14] and high strength (contraction force stress up to 50 MPa) [14], quick response (at chosen conditions of kHz frequency) [15] and biocompatibility [6,16]. Conducting polymer like polypyrrole (PPy), polyaniline and poly(3,4-ethylenedioxythiophene) (PEDOT), which undergo volume changes during electrochemical oxidation and reduction, are excellent materials for actuators.

3.2.1 Actuation mechanism

The actuation of CP based IEAPs is based on double layer charging-discharging and redox processes [12]. The actuation voltage is at least an order of magnitude lower than that required for electronic EAPs, making them an appealing competitor.

An actuation of CPs is caused by electrochemical change in the oxidation state of the polymer chain and the movement of electrolyte ions upon applying electrical potential (Figure 2). The ingress and egress of ions and their solvate shells between the polymer matrix and the associated electrolyte to balance the charge causes swelling or contraction of the polymer, which alters the mechanical properties of the CP and leads to macroscopic volume change. In the case of a single CP film, the volume change manifests in a linear movement (Figure 4): the CP film expands and compresses when changing the polarity. CP-based bending actuators are typically tri-layers with 2 CP films on the opposite sides of the electronically insulating but ion permeable membrane (Figure 2). On opposite electrodes, opposite redox processes take place: bending is a result of the unequal expansion of both electrodes, regardless of the polarity of the applied voltage [18]. The membranes of such tri-layer actuators serve as an electrolyte reservoir (ion permeable) and actuators are therefore able to operate outside of electrolyte media making them attractive from the perspective of practical applications. Such a design transforms a relatively small strain difference into large deflections when large forces are less important than large strokes [12].

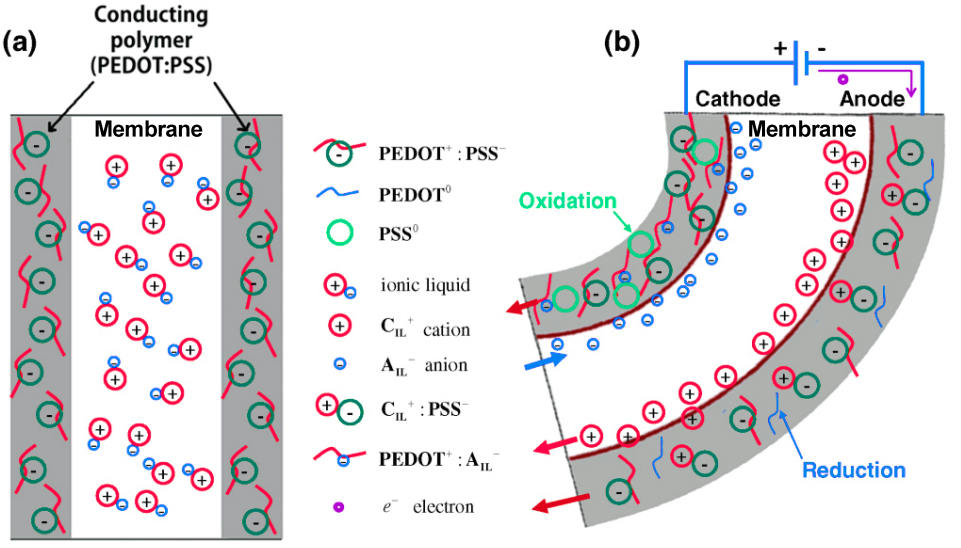

Figure 2. Scheme of the actuation mechanism of the conducting polymer [17] actuator in its steady state (a) and under applied voltage (b). From [17] with modifications[1]

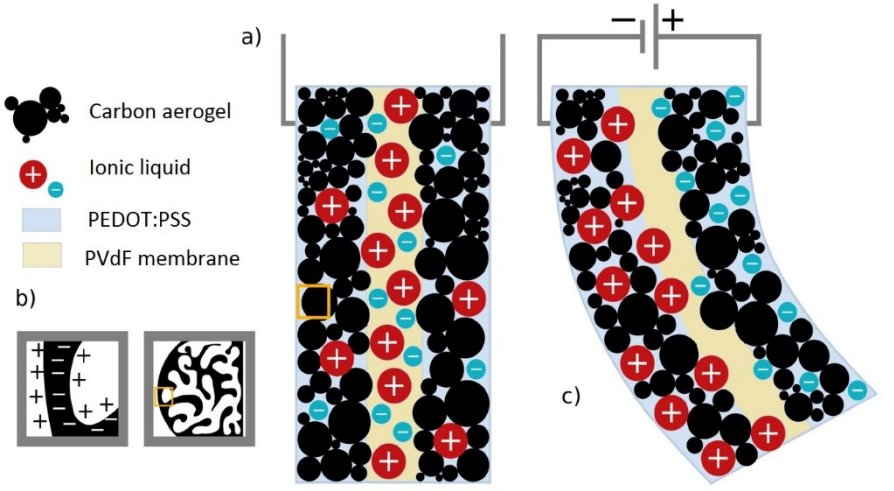

Figure 3. A schematic depiction of an actuation based on electric double layer formation – a characteristic mechanism for carbon-based actuators. (a) and (c) depict an actuator at neutral state and under applied voltage respectively. (b) Simplified notation of electrical double-layer formation inside porous carbon media. Image from (Torop et al. 2012) with modifications.

[1] Electro-active hybrid actuators based on freeze-dried bacterial cellulose and PEDOT:PSS. Kim, Si-Seup; Jeon, Jin-Han; Kee, Chang-Doo; Oh, Il-Kwon. *Smart Materials and Structures,* **22,** 085026. © IOP Publishing. Reproduced with permission. All rights reserved.

Depending on the relative sizes of anions and cations (including the solvation shells), anion charge, density of the CP structure, etc., CP actuators can be anion active (Figure 4a), cation active (Figure 4b) or mixed type. Usually, large anions have low diffusion speed or are immobile inside the polymer matrix, and the redox process charges are compensated by the more mobile cations. Otherwise, electroneutrality is maintained by anions entering and leaving the active CP material [12].

It is possible to enhance the capacitive properties and energy efficiency of the actuator [19] by adding carbon to the conducting polymer (Figure 3) and making carbon-conducting polymer-composite electrodes.

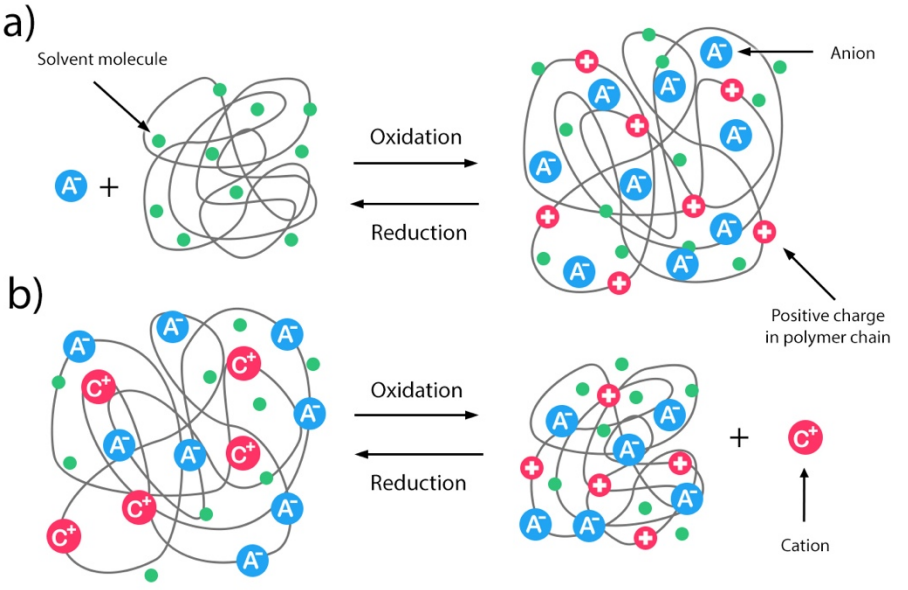

Figure 4. Linear actuation in electrolyte solution (a) anion active and (b) cation active actuation

Air operated actuators often suffer from solvent evaporation and need encapsulation for long-term operation. Alternatively, room temperature ionic liquids (ILs), which have negligible vapor pressure, can be used [20]. In the current work, IL was chosen as an electrolyte for bending mode actuation in air. [EMIm][TfO] was selected due to compatibility with the applied hydrophilic PVdF membrane and aqueous conducting polymer suspensions. In addition, IL is a non-volatile electrolyte and the solvent evaporation is not a factor that influences the electromechanical properties during actuation.

3.2.2 Architecture of the actuator

In IEAP actuators with trilayer configuration, two ion and electron conductive electrodes are separated by an ion conductive membrane. Examples of currently used membrane materials in the IEAP actuators are PVdF (Figure 5d) and its derivatives [21,22], NBR/PEO based interpenetrating networks [23], chitosan [24] and cellulose derivatives [17]. The membrane of the actuators has a dual function: it serves as electrolyte storage and an ion conductive electronic separator layer for tri-layer air-operated bending actuators and as a mechanically supporting interlayer for linear actuators. In this work, the membrane also acted as a substrate onto which the CP based electrode layers were printed.

The layered structure needs good electrical and mechanical contact between the layers and between the active material and the driving power supply. A hydrophilic modified PVdF membrane was used for deposition of aqueous CP colloidal solution. The commercial PVdF is relatively homogeneous compared to in-house fabricated membranes and it is widely studied in actuator configuration, making the effects of electrodes on the actuator properties distinctive.

Electrodes peel off from unmodified hydrophobic PVdF PEDOT:PSS and make the actuator unable to perform. Simate et al [25] had an approach to making the surface of the hydrophobic PVdF hydrophilic using polyethylene glycol methacrylate (PEGMA) solution and subsequent plasma treatment. In the current work, the adhesion problem was solved by using a commercial hydrophilic PVdF (Millipore Durapore, hydrophilic, thickness 110 µm, pore size 0.1 µm, porosity 70%), which also enabled the author to compare the effect of printed electrodes on the actuator without considering the variations in the membrane quality (publication I and II).

An interpenetrating network of NBR/PEO [15] was also used for miniaturisation of the CP-based actuator (Publication III).

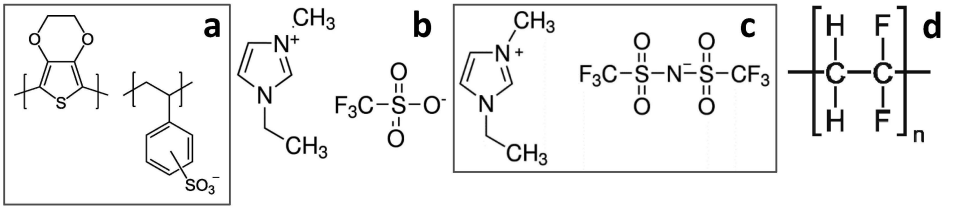

Figure 5. Structural formula of (a) PEDOT:PSS, (b) [EMIm][TfO], (c) [EMIm][TFSI], (d) and PVdF

IEAP films can be applied to substrates using a number of methods. If the polymer can be dissolved or dispersed in a solvent, then it can be cast [26,27], spray-coated [28,29] or spin coated [30–32]. The polymers can likewise be applied to a substrate if it is melt-processable [33]. If the polymer has a soluble precursor or precursor monomer, then that can be applied to the substrate and cured, such as by heating, to form the conjugated polymer. Alternatively, it is

possible to UV-crosslink a precursor with a photo-initiator or photo acid generator [33]. There are several ways to deposit films from an unmodified monomer solution. Chemical vapor deposition has been used for poly(p-phenyl-enevinylene) (PPV) [34] and for polypyrrole (PPy) [35]. A solution of the monomer, an oxidiser and an inhibitor can be applied to the substrate and the mixture heated to drive off the inhibitor, allowing the polymerisation to take place on the wafer. Poly(3,4-ethylenedioxythiophane) (PEDOT) can be deposited with this method [15]. If the polymer is insoluble and can't be melted, and none of the above can be applied, then electropolymerisation is an industrially used alternative [21,33]. These methods however cannot be used directly for fabrication of micro-actuators or for applying patterned CP films.

4. INK-JET PRINTING TECHNOLOGY FOR IEAP FABRICATION

When using the methods described in the previous chapter for CP film fabrication, the miniaturisation and patterning are carried out by cutting, for example via laser cutting [15,36] and masking [37]. Printing technology for IEAP fabrication was first reported by [25] as an alternative. The technology allows the deposition of polymeric patterns onto different surfaces without the drawbacks, in terms of cost, time and process flexibility, that could derive from other traditional techniques (spin coating and casting). In addition, three-dimensional structures can be fabricated by depositing layers on top of the other [38]. Ink-jet printed piezoelectric polymer actuators have been made by [39], [40]. Ink-jet printing in the EAP domain is an evolving field. Miniaturisation and patterning combined with printed electronics can produce innovative micro-applications for example in the soft robotics field.

4.1 Inkjet printing technology

Drop-on-demand inkjet printing is a digital printing technique. The desired structures can be printed directly from a software-generated design and no masking is required. Film formation is dependent on the surface energy of the substrate where the ink is deposited and its interactions with the ink. These aspects make inkjet printing a very flexible technique. In addition to printed electronics, organic photovoltaic devices [41–43], organic light-emitting devices [44], memory devices [45], organic transistors [46] and RFID devices [47] have been fabricated using inkjet printing.

Inkjet printers operate either in continuous or drop-on-demand (DOD) mode. In continuous-mode inkjet printing (Figure 6a), the ink is pumped through a nozzle to form a liquid jet. Uniformly spaced and sized droplets are obtained by applying a periodic disruption, leading to jet break-up. Continuous-mode inkjet printing is mainly used for high speed graphical applications such as textile printing and labeling. The DOD method (Figure 6b, Figure 6c) has a smaller drop size and higher placement accuracy compared to continuous mode inkjet printing. An acoustic pulse ejects ink droplets from a reservoir through a nozzle. The pulse can be generated either thermally or piezoelectrically. In a thermal DOD inkjet printer (or bubble-jet) (Figure 6b), ink is heated locally to form a rapidly expanding vapor bubble that ejects an ink droplet. Thermal DOD usually uses water as a solvent and may therefore impose restrictions on the number of polymers that cannot be printed using this technique, although non-aqueous thermal inks are available. Heating can also damage some polymer structures or biomaterials (cell cultures) if there is a need to print them concurrently with the polymer solution. Piezoelectric DOD inkjet printing (Figure 6c) on the other hand relies on the deformation of some piezoelectric

material to cause a sudden volume change and hence generate an acoustic pulse. Piezoelectric DOD is, in principle, suited to a variety of solvents [48] and the latter was also used in this work.

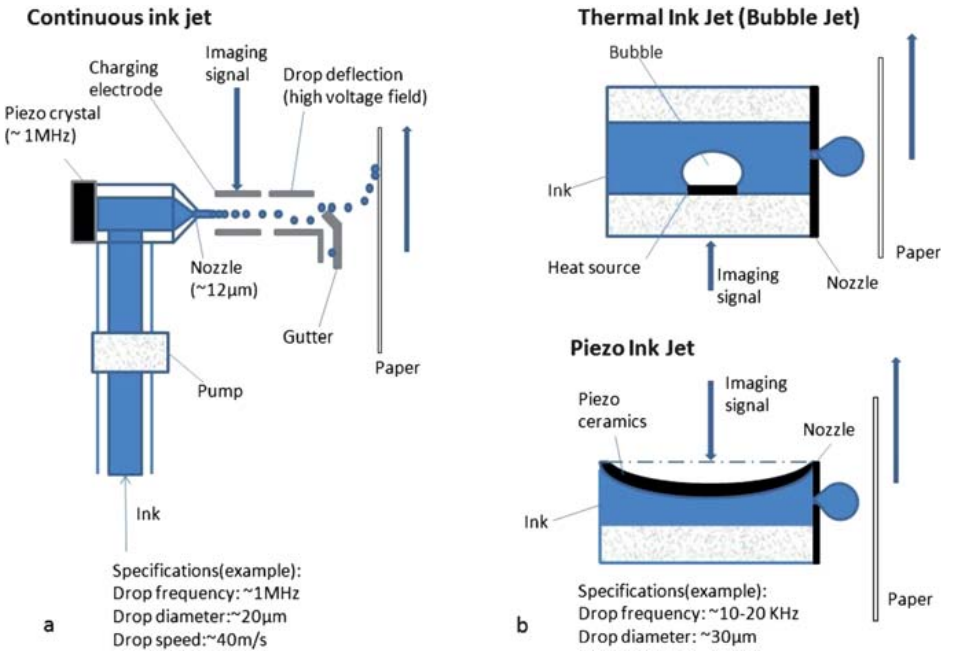

Figure 6. Inkjet technology: (a) continuous inkjet printing; (b) 'drop on demand' inkjet printing [49][2]

Polymers can be printed from the melt when the complete inkjet system is heated. This technology is used in the graphical industry for printing waxes. Another possibility for inkjet printing of polymers is represented by the utilisation of colloidal suspensions of polymer lattices, which has the advantage of presenting a high-molecular-weight polymer in a low-viscosity form. This possibility was used for deposition of CP in this work.

The elaboration of printable actuator membranes was not the focus of the current research; nevertheless, polyvinylidene fluoride-trifluoroethylene (PVdF-TrFE) has recently been printed by [50] and its applications have been suggested for actuators.

In deposition by inkjet printing there are requirements for the viscosity and surface tension of the ink. For jetting, the viscosity of the ink should be suitably low, depending on the printer but typically below 20 mPa [51]. When too high, kinetic energy is viscously dissipated and no droplet is ejected. Eventual polymer solutions should therefore be sufficiently dilute. The shear rates

[2] Republished with permission of Royal Society of Chemistry, from *The Analyst*, Printing conducting polymers, Weng, B.; Shepherd, R. L.; Crowley, K.; Killard, A. J.; Wallace, G. G., **135,** ©2018, permission conveyed through Copyright Clearance Center, Inc.

involved in inkjet printing are, however, in the order of 10^5 s^{-1}; hence shear-thinning may occur. For a given pressure wave at the nozzle, the lower the viscosity the greater the velocity and the amount of liquid propelled forwards, which leads to the formation of long tails behind the head of the drop. The surface tension is responsible for the spheroidal shape of the liquid drop emerging from nozzle.

In designing the patterns for the microprinter, limiting factors have to be considered; for example width of one line is determined by the particle sizes in the ink as well as the orifice diameter of the nozzle of the printhead. The particle size should be equal to or less than 10% of the orifice diameter. How miniature the print can also be dependent on the accuracy and repeatability of the used printer.

Finally, the wetting behavior of fluid and nozzle material is of importance as wetting of the nozzle outlet face results in spray formation [51].

4.2 Suspensions of conducting polymers

Conductive polymers films for IEAP actuator fabrication are synthesised in house on top of the membrane substrate using chemical or electrochemical polymerisation [15,21]. In case of commercial conducting polymer inks, the previously synthesised polymer film can be applied directly on to the membrane without having extra steps. For example, to make electrodes with electrochemical polymerisation on the membrane, it has to be sputtered with gold to make it conductive. Printing CP inks is therefore less time consuming, with fewer fabrication steps.

A commercial conducting polymer ink was chosen for electrode material: a colloidal solution of poly(3,4-ethylenedioxythiophene) polystyrene sulfonate (PEDOT:PSS) (Clevios™ P Jet 700, solids content 0.61.2 wt %, Heraeus Precious Metals GmbH & Co. Germany). 3,4-Ethylenedioxythiophene (EDOT) is chemically polymerised in a PSS solution to give a PEDOT:PSS (Figure 5a) water emulsion. The conjugated polymer PEDOT is positively doped, and the sulfonate anionic groups in PSS are counter ions used to balance the doping charges [52]. Its aqueous dispersion was first commercialised under the trade name of Baytron® by Bayer AG, then by H.C. Starck and currently by Heraeus under the trade name of Clevios™.

The commercially available PEDOT:PSS aqueous dispersion is a deep-blue opaque solution with high conductivity and thermal stability. It readily forms a continuous thin film on either rigid or flexible substrates by various solution-processing techniques including spin casting, doctor blade, slot die coating, spray deposition, inkjet printing, screen printing, etc. [53] The PEDOT:PSS film is smooth and has a surface roughness generally less than 5 nm (deposition technique dependent). PEDOT:PSS exhibits a wide range of electrical conductivities from 10–2 to 103 S cm–1, influenced by synthetic conditions, processing additives or post-treatment. PEDOT:PSS films have a high work function of 5.0–5.2 eV. The superior conductivity and high work function can often induce

spontaneous charge transfer with fast kinetics, thus providing PEDOT:PSS with catalytic properties. Physically and chemically, PEDOT:PSS possesses good photo- and electrical-stability in air. Owing to the above-mentioned properties, PEDOT:PSS or PEDOT with some other dopant have been found in a wide range of applications in energy conversion and storage fields [53] and can be suitable electrode material for IEAP actuators.

4.3 Strategy of printing and actuator preparation

The printer used in this work was jetlab®II Precision Printing Platform from MicroFab Technologies Inc. (accuracy ±15 µm, repeatability ±5 µm). Equipped with a downwards-looking camera, the alignment of printed features can be inspected and adjusted. MJ-AT-01 drop-on-demand single jet dispensing devices with 50 µm orifice diameter were used. The small particles of the polymer or its monomer dissolved in a volatile solvent, which is ejected drop by drop onto the substrate. Fluids with viscosity of less than 20 cPs and surface tension in the range of 20–70 dynes/cm can be dispensed [54].

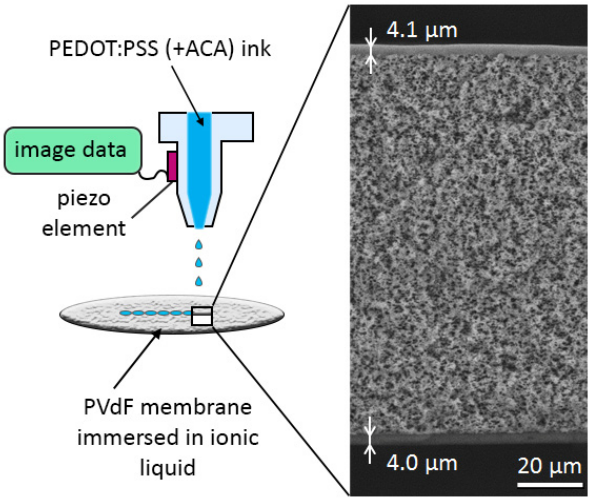

Figure 7. Scheme of the actuator fabrication with SEM insert from the cross-section of the actuator

A 2-ml fluid reservoir was filled with either PEDOT:PSS ink or PEDOT:PSS-ACA (activated carbon aerogel) ink: 0.7% ACA was added to the commercial solution, and the mixture was sonicated with an ultrasonic probe for 15 min and then filtered before printing.

The jetting frequency was 700 Hz with application of a customised waveform. The temperature of the substrate holder was set to 45 ºC to enhance evaporation of the solvent. Patterns of 2 × 20 mm rectangles were designed and exported in bitmap monochrome format to be loaded by the printer software.

To avoid CP particles from submerging too far into the membrane and inducing shorting, the membrane was saturated with IL. The PEDOT:PSS based actuator electrodes were printed on both sides of the membrane, aligned to each other (Figure 7) and then cut out of the membrane with a scalpel. In publications I and II, PVdF membrane was used.

Semi-IPN NBR/PEO membrane was chosen as a membrane (8 µm) for microactuator fabrication (Figure 8), as it was proven to work in other microactuators [15]. Spin coating is an established technology for NBR/PEO membrane fabrication and was utilised to make homogeneous and thin films (supplementary material in the work of Maziz et al [15]). Spin coated NBR/PEO membrane was too thin to be self-supporting; therefore, Teflon was used as an additional supporting substrate and the actuators were fabricated as presented in Figure 8: sacrificial polyvinyl alcohol (PVA) layer and NBR/PEO layer were spin coated on top of each other on a microscope slide. Conducting polymer electrodes of PEDOT:PSS ink were printed on top of the NBR/PEO layer. Then the sacrificial layer was dissolved in a water bath and the membrane with printed electrodes on one side was flipped and supported on a Teflon surface. Thereafter, the second PEDOT:PSS electrodes were printed on the opposite side of the membrane.

The current work compares IEAPs with printed CP and CP-carbon composite based actuators, where carbon content in the PEDOT:PSS ink is 0.7 wt %. Microactuators with semi-IPN NBR/PEO membrane were prepared only with PEDOT:PSS ink. The thickness of the electrodes was varied with differing numbers of layers printed on top of each other.

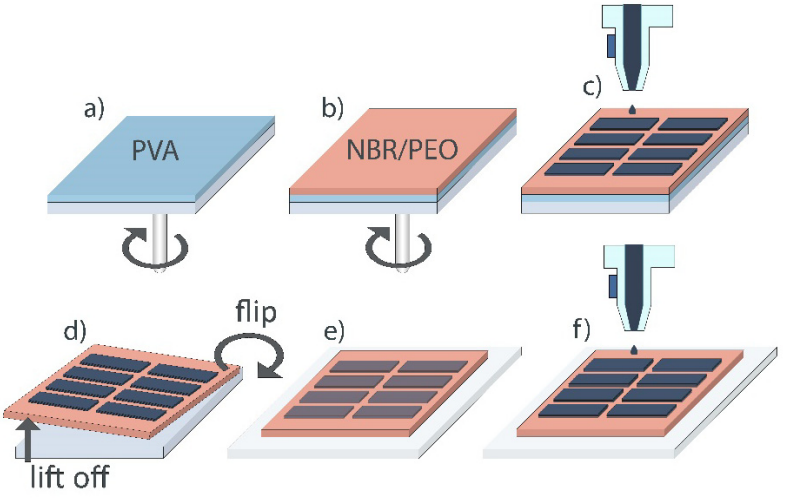

Figure 8. Scheme of actuator fabrication with spin coated NBR/PEO membrane and printed electrodes: (a) spin coated sacrificial PVA layer, (b) spin coated NBR/PEO layer, (c) printed electrode layers, (d) dissolution of PVA layer in water and flipping of the composite, (e) Teflon supported flipped composite, (f) printing layers of PEDOT:PSS electrode to the other side of the membrane

4.4 Characterisation of the actuators

Electrode stress, strain, capacitance, thickness of the actuator and elasticity were analysed to examine the implementation of ink-jet printing technology on the fabrication of the actuator and their fabrication repeatability.

4.4.1 Mechanical properties

The thickness of the actuator and its electrodes and the morphology of the PEDOT:PSS and PEDOT:PSS-ACA electrodes was studied under SEM (TM3000 Hitachi High-Technologies Corporation, Japan). For cross-sectional images, the actuators were broken in liquid nitrogen. The thicknesses were determined using SEM tools.

To determine the effect of different electrode thicknesses on elasticity of the actuator, equivalent bending elastic modulus E was calculated according to Equation 1, Kiesewetter et al [55]:

$$E = 48\pi^2 \rho f_r^2 l^4 \lambda_t^{-4^-} h^{-2}, \quad (1)$$

where ρ is the density of the actuator, f_r is the resonance frequency, l is the free length of the actuator, λ_t is the eigenvalue (where t is an integer that describes the resonance mode number; for the first mode $\lambda_1 = 1.875$) and h is the thickness of the actuator.

4-point probe was used to measure surface resistance.

3.7.2 Electromechanical and electro-chemo-mechanical properties

Electromechanical and electrochemical analysis of the actuators was performed in both linear and bending actuation mode. Three-layered actuators with an ion-permeable separator in the middle are usually used in bending mode, but the three-layered structure can also be used in linear mode, where the membrane is in a supporting role.

Bending actuation mode

EC measurements were performed using [EMIm][TfO] as the electrolyte.

In bending mode, the actuator is sandwiched between the oppositely charged electrodes that produces potential change where ions start to move to compensate for the charge in the electrodes.

Strain difference is a measure usually used to describe the bending properties of the actuators to make them comparable with the other type of actuators. The strain difference – is calculated from the displacement signal using Equation 2 [56]:

$$\varepsilon = \frac{2 * d * h}{L^2 + d^2} * 100\ \% \qquad (2)$$

where, d is half of the peak-to-peak displacement, h is the thickness of the actuator and L is the measurement distance from the fixed input contacts, as illustrated on Figure 9.

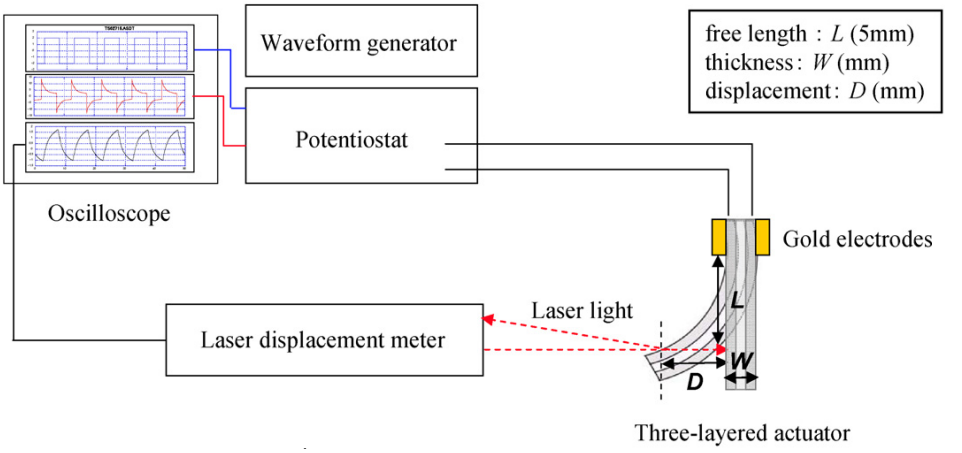

Figure 9. Bending setup [56][3]

EC measurements of bending actuators were conducted in two-electrode configuration with potentiostat/galvanostat PARSTAT 2273. Printed membrane sides, clamped between gold plates, were used as electrodes connected to working/sense and counter/reference inputs, respectively.

Electro-chemo-mechanical parameters of the bending actuators were characterised using an in-house setup with custom NI Labview software interfaced through PCI-6036E DAQ (National Instruments) with a laser displacement meter LK-G82/LK-G3001P (Keyence). The current of the actuation signal was measured using an in-house current amplifier/zero resistant ammeter (ZRA). Actuators were placed side-ways (5 mm clamped, free length 15 mm) between flat gold contacts (Figure 9). The displacement measurement distance from the clamped end of the actuator was adjusted using an XY-micrometer stage.

A Microforce Sensing Probe with a sensor force range of ±1000 μN was used for blocking force measurements in bending mode (Figure 10). The response to the actuation frequency was obtained by applying an exponential chirp potential signal (0.01–50 Hz, ±1 V, 100 s) to the actuator, followed by Fast Fourier Transform-based spectral computations.

[3] Reprinted from *Sensors and Actuators, B: Chemical*, Actuator properties of the complexes composed by carbon nanotube and ionic liquid: The effects of additives, Sugino, Takushi; Kiyohara, Kenji; Takeuchi, Ichiroh; Mukai, Ken, Asaka, Kinji, , **141**, 179-186, Copyright (2018), with permission from Elsevier

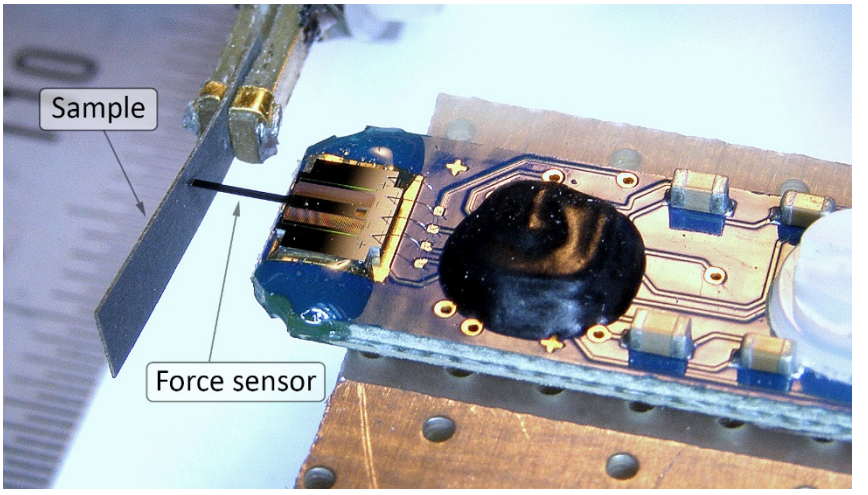

Figure 10. Force measurement setup. Sensing probe placed 3 mm from the clamp (effective length) against the sample

Linear actuation mode

The actuator is sandwiched between clamps with the same charge electrodes (working electrode) and the counter and Ag/AgCl reference electrode in the electrolyte solution (Figure 11). The voltage at the actuator clamp, the current and the displacement were measured simultaneously. The three-electrode cell shows exactly at which potential a reaction occurs compared to the reference electrode, but the cell has to be in the electrolyte solution; it cannot be operated in air.

One end of the trilayer samples was fixed on a force sensor (Figure 10). The other end was connected to a fixed arm equipped with platinum contacts that connected the outer layers of the trilayer. The trilayer served as the working electrode in the linear actuator analyser setup, with a platinum sheet as the counter electrode and an Ag/AgCl wire as the reference electrode. The fixed sample was immersed in the measurement cell that was filled with the electrolyte. The in-house ECMD [28] measurement setup is different from commercial devices because it uses a movable force sensor instead of a fixed sensor. This setup can determine how much mass (mg) is needed to change the length of the film by 1 μm (k-factor: mg μm−1). The initial length of the films between the clamps was 1 mm. The force (isometric, constant length) and length changes (isotonic, constant force of 4 mN) as well as the applied electrical signal were measured in real time with in-house software. Cyclic voltammetry and chronoamperometry at frequencies of 0.0025 Hz, 0.005 Hz, 0.01 Hz, 0.025 Hz, 0.05 Hz and 0.1 Hz were performed within a voltage range of 1 V to –0.6 V.

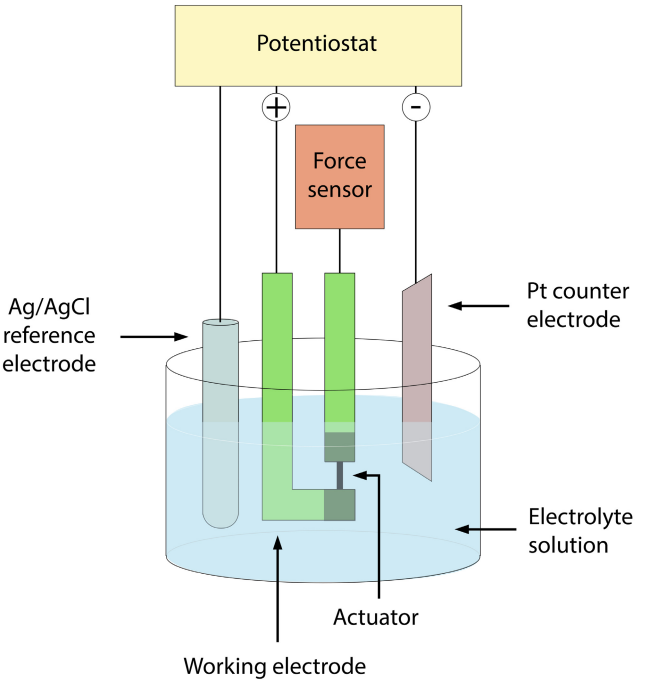

Figure 11. Scheme of the linear muscle analyser with a force sensor and integrated self-written software, potentiostat and three-electrode measurement cell

Isometric and isotonic cyclic voltammetry electro-chemo-mechanical deformation (ECMD) measurements were conducted to determine the stress and strain of the actuator in linear actuation mode (Figure 11). ECMD was also used to determine whether the composite in a given solution is cation- or anion-driven. The effect of added ACA was also observed.

From the results of ECMD measurements, ion transport was investigated by determining the diffusion coefficients. The diffusion coefficient also allows the evaluation of the rate of ion exchange as reflected in the actuation rate. The electrochemically stimulated conformational relaxation (ESCR) model includes both electrochemical and polymeric structural aspects expressed by Equation 3:

$$\ln\left[1-\frac{Q}{Q_t}\right]=-bt, \tag{3}$$

where Q_t is the total charge consumed during the time t, calculated over the integration of the current-time curve of the chronoamperometric experiment, and Q is the charge consumed at each point of the time. The diffusion coefficient D is included in b (h is the thickness of the sample), Equation 4:

$$D = \frac{bh^2}{2} \tag{4}$$

The slope of $ln\left[1 - \frac{Q}{Q_t}\right]$ versus t allows the diffusion constant to be calculated (Equation 4). The relation is valid under conditions where the polymer expands on reduction, increasing the rate of ion diffusion [57], and shrinks at the beginning of oxidation (cation diffusion kinetic control).

To evaluate the specific capacitance C_s of linear actuators, the slope ($\Delta E/\Delta t$) values at the chronopotentiometric curves at discharge (after the IR potential drop correction) were used according to the Equation 5:

$$C_s = I/\left(-\frac{\Delta E}{\Delta t} * m\right), \tag{5}$$

where I is the applied current (A) and m is the mass (g) of the electrodes.

Most studies of actuators based on trilayer design with inkjet printed conducting polymer electrodes have been conducted in the bending mode in air, using ILs as nonvolatile electrolytes [25]. Little attention has been paid to the role of the electrolyte solution in such devices. In publication III, the effect of solvent on the actuation of PEDOT:PSS-semi-IPN trilayer was investigated in linear mode, with samples immersed in electrolyte in a three electrode configuration (Figure 11).

For ECMD measurements, the electrochemical window is in the potential range of –0.6 to 1 V for PVdF based actuators and –0.6 to 0.65 V for NBR/PEO based actuators. Those limits are set to avoid irreversible faradaic processes.

5. RESULTS AND DISCUSSION

5.1 Control over electrical, mechanical and electromechanical properties of the actuators

The PEDOT:PSS ink is sold as an electron conductive polymer. In this work it is shown that it can be also applied to processes utilising electrochemical processes. To see the changes in the actuator caused by different electrode thickness, different number of layers of CP and CP-carbon composite electrodes were printed on top of the commercial PVdF membrane.

The prepared samples were printed with 5, 10 and 20 layers of PEDOT:PSS ink and compared with those with 5, 10 and 20 layers of PEDOT:PSS-ACA ink, denoted as P5, P10 and P20 and A5, A10, A20, respectively. It can be measured from the cross-section SEM images (Figure 13) that the growth of the layers is cumulative. The increasing number of printed layers is in linear correlation with the thickness of the electrode h_e, where one layer of printed electrode (Table 1 h_1 and Figure 12) adds 360 ± 26 nm for PEDOT:PSS and 550 ± 50 nm in the case of PEDOT:PSS-ACA. Thinner films have been obtained using spin coating [32], but the thickness variation ranged from 6 to 23 µm with spin coating carbon-polymer electrode solution [31].

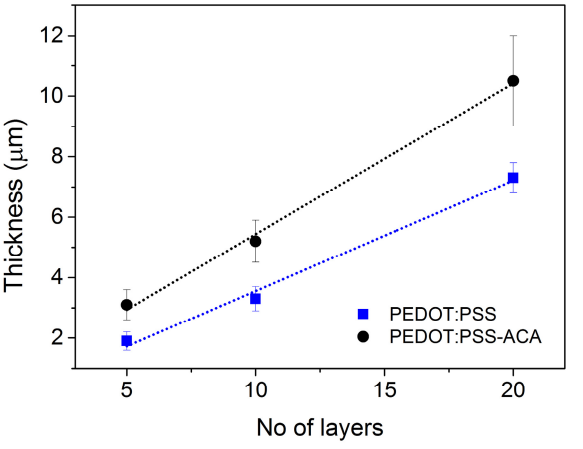

Figure 12. Added layers and thickness correlation for PEDOT:PSS and PEDOT:PSS-ACA electrodes

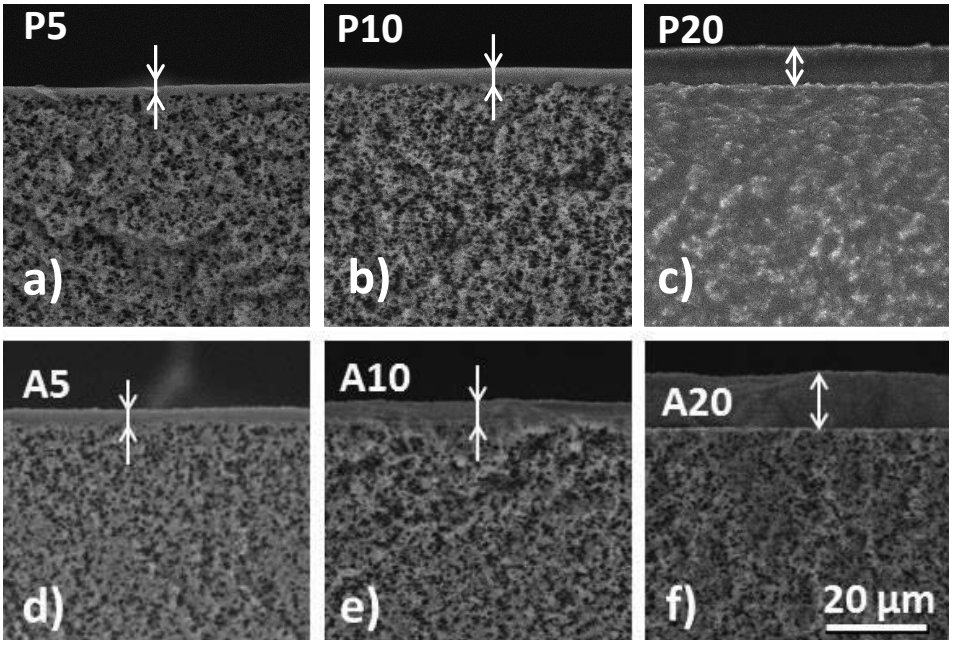

Figure 13. SEM image of cross-section of printed PEDOT:PSS (P5, P10, P20) and PEDOT:PSS-ACA (A5, A10, A20) electrodes with 5, 10 and 20 layers on IL-saturated PVdF membrane, respectively. The electrode thickness is marked with arrows. The electrodes on the opposite side of the membrane (not shown on this image) have the same thickness as on the side shown on this image

Table 1. Physical parameters of printed electrodes

Sample	*No. of printed layers*	h_e *(µm)*	h_1 *(nm)*	*m (µg)*	$R_{s\,IL}$ $(\Omega \cdot sq^{-1})$*	R_s $(\Omega \cdot sq^{-1})$*
P5	5	1.9 ± 0.3	380 ± 60	91 ± 21	64 ± 9	–
P10	10	3.3 ± 0.4	330 ± 50	167 ± 14	22 ± 4	63 ± 8
P20	20	7.3 ± 0.5	370 ± 30	362 ± 21	12 ± 2	16 ± 1
A5	5	3.1 ± 0.5	600 ± 100	132 ± 21	53 ± 12	195 ± 14
A10	10	5.2 ± 0.7	520 ± 70	222 ± 64	22 ± 2	96 ± 5
A20	20	10.5 ± 1.5	520 ± 80	447 ± 127	14 ± 3	34 ± 8

Sheet resistance (R_s) and sheet resistance when saturated in IL ($R_{s\ IL}$) both decrease when the thickness of the electrodes increases in the range of 5 to 20 layers of CP ink. The rate of resistance decrease between 10 and 20 layers is lower compared to that between 5 and 10 layers. The sheet resistance should not be thickness dependent and therefore the decrease of R_s and $R_{s\ IL}$ indicates that the electrical properties of the electrodes can be further improved by increasing electrode thickness. However, the increase in electrode thickness has a direct effect on the elastic modulus of the actuator (Table 2).

Table 2. Equivalent bending elastic moduli of PEDOT:PSS and PEDOT:PSS-ACA actuators with 5, 10 and 20 layers of printed electrodes based on the mechanical (E_M) and electromechanical (E_{EM}) resonance frequencies

Sample	E_M *(MPa)*	E_{EM} *(MPa)*
P5	226 ± 12	95
P10	263 ± 20	88
P20	318 ± 6	79
A5	124 ± 9	220
A10	156 ± 14	230
A20	177 ± 6	242

The equivalent bending elastic moduli were calculated from the resonance frequency of mechanical actuation and electromechanical actuation. The equivalent bending elastic modulus of the applied dry commercial PVdF membrane, calculated based on the mechanical resonance frequency, was 290 MPa and 100 MPa when saturated with IL. The modulus of the actuators depended on whether or not the voltage was applied to the actuator. Applied potential decreases the stiffness of the CP-based composites. This correlates with the findings of Alici and Higgins [2], attributing it to changes in the polymer backbone, plasticisation effects or mechanisms of electrical activation. Elastic modulus decreased with the increasing number of printed layers of CP-ink (P5-P20, A5-A20), except in the case of PEDOT:PSS (P5-P20), which is determined by electromechanical (E_{EM}) actuation. That is associated with Joule heating of the actuator during actuation.

It was confirmed that ink-jet printing allows consistent deposition of the electrode material on ion permeable membrane. Besides the electrode thickness, the layer-wise growth of CP and CP-ACA electrodes influences electrical, mechanical and electromechanical properties of the resulting actuators. Both, PEDOT:PSS and PEDOT:PSS-ACA-composite proved to be suitable for fabrication of electrode films in a reproducible manner and it can successfully be applied to manufacturing of actuator electrodes, thus opening the door for additive manufacturing of soft actuators with complex patterning. The controlled growth of actuator electrodes is addressed in publication II.

5.2 Electromechanical properties

In addition to previously described mechanical properties, the thickness of the electrodes also influences the electromechanical properties.

The electromechanical properties of the three-layered conducting polymer-ion conductive membrane composites were studied in bending and in linear actuation mode (publication I and II respectively). [EMIm][TfO] (Figure 5b) was used as an electrolyte in bending mode actuation in air. 0.2 M Li[TFSI] in PC was used as

an electrolyte for linear actuation and in the case of NBR/PEO membrane based actuators, 0.2 M Li[TFSI] aqueous solution was additionally used.

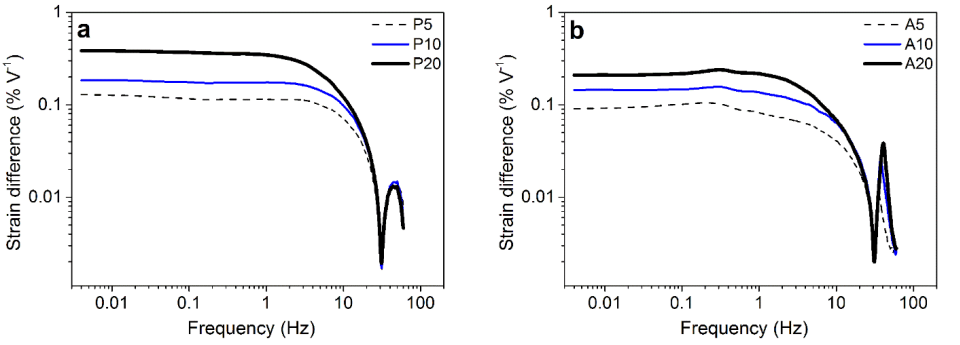

Figure 14. (a) Bending strain difference of PEDOT:PSS and (b) PEDOT:PSS-ACA on PVdF (exponential chirp potential signal ±1 V, 0.001 – 60 Hz.

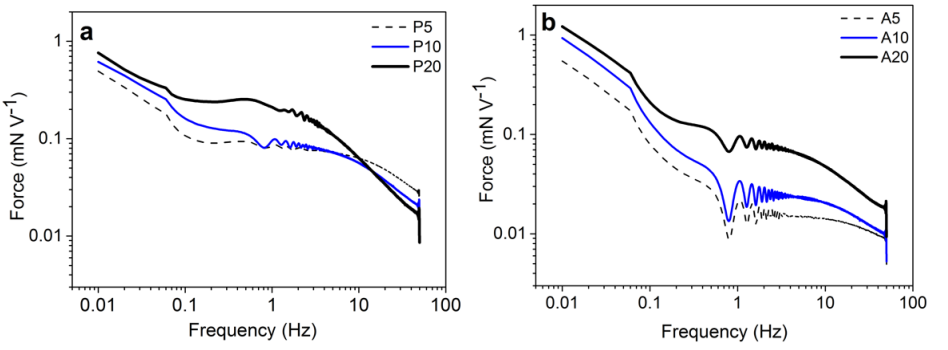

Figure 15. (a) Blocking force in bending mode of PEDOT:PSS and (b) PEDOT:PSS-ACA on PVdF (exponential chirp potential signal ±1 V, 0.01 – 50 Hz)

Figure 14 shows that actuation is frequency dependent at higher frequencies. In the range 0.001–2 Hz, the strain difference stays constant and then sharply decreases until an electromechanical actuation resonance frequency occurred at 45 Hz. Similarly, the blocking force (Figure 15) is frequency dependent: in the range of 0.001–2 Hz, the blocking force gradually decreased with a plateau from 0.04 to 1 Hz. In the range of 5–20 layers, the strain is increasing with the thickness. Despite the thickness of the electrodes in samples being different, the frequency dependence is similar for the actuators and the resonant frequencies coincide in the same material. The actuators with ACA incorporated in the CP film have higher E_{EM} and are therefore able to utilise a higher force (Figure 15) at lower frequencies. The bending experiments showed a cation active actuation – at oxidation, the CP film contracts and bending towards the positive electrode occurs.

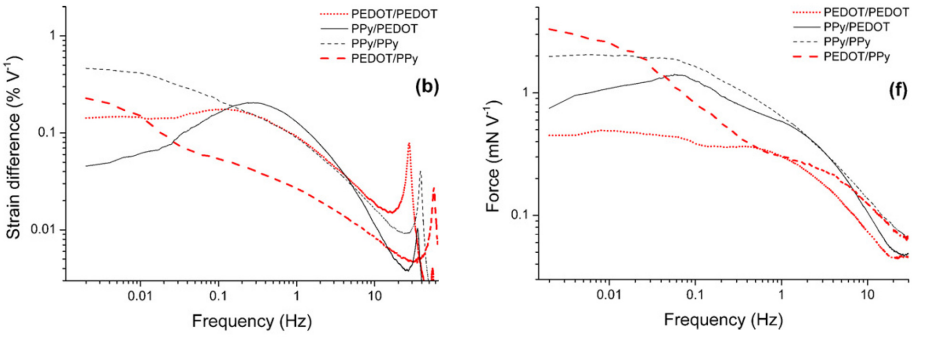

Figure 16. (b) Bending strain difference for electrochemically deposited electrodes on PVdF and (f) generated force. [EMIm][TFSI] as electrolyte [21][4]

Ionic electromechanical actuators with electrochemically polymerised CP electrodes on PVdF membrane fabricated by Temmer, et al. [21] have comparable strain difference and force range (Figure 16) as the ones fabricated in this work (Figure 14, Figure 15). When comparing PEDOT:PSS actuator P20 (electrode thickness 7.3 µm) with PEDOT-based (5.3–12.5 µm) actuators from [21], it can be seen that the strain difference and force are even outpaced. With printed electrode actuators, the strain is frequency independent (0.001 Hz to 1 Hz) which is beneficial for applications that need stable actuators.

Fabricating conducting polymer actuators from stable commercial PEDOT:PSS ink reduces the fabrication time and number of steps (polymerisation done already in the factory and there is no need to make the membrane conductive for electrochemical polymerisation).

The same tri-layer configuration was used in the linear actuation mode, using 0.2 M Li[TFSI] in PC, to study the electrochemical behavior in the actuator. Again cation active actuation took place. When applying a positive charge to the working electrode, the volume of the actuator decreases – Li^+ moves out of the CP matrix to compensate for the charge and between the clamps the increase in force is registered.

Electromechanical actuation of PEDOT:PSS based actuators with [EMIm][TfO] as the electrolyte are cation driven – the contraction of PEDOT:PSS occurs at oxidation, where the (positive) electronic charge on the polymer is compensated by the egression of cations. At reduction, the opposite process occurs, and the volume of the electrode expands.

[4] In search of better electroactive polymer electrode materials: PPy versus PEDOT versus PEDOT-PPy composites, Temmer, Rauno; Maziz, Ali; Plesse, Cédric; Aabloo, Alvo; Vidal, Frédéric; Tamm, Tarmo, *Smart Materials and Structures,* **22**, 104006. © IOP Publishing. Reproduced with permission. All rights reserved.

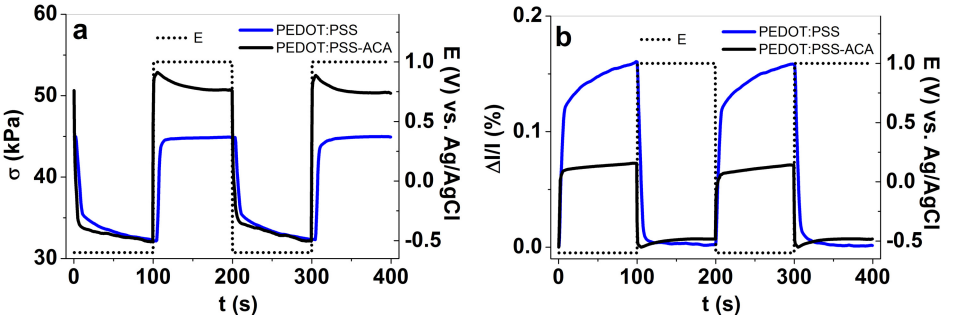

Figure 17. Linear stress (a) and strain (b) of PEDOT:PSS and PEDOT:PSS-ACA on PVdF membrane

At oxidation (Figure 17a), the stress increases with the potential (Figure 17a), followed by a slow relaxation on reduction. The isotonic length change curves (Figure 17b) show a continuous increase of strain upon reduction.

Some micro devices might need a higher force and stiffer manipulators; for that purpose carbon was incorporated into CP matrix. The synergistic effects of conducting polymer-carbon actuators have also been confirmed by [19,58].

5.3 Influence of conducting polymer-carbon-composite electrodes on actuator properties

In this work, actuators with hybrid conducting polymer-carbon electrodes, PEDOT:PSS-ACA, were studied in parallel with PEDOT:PSS actuators. As shown in Figure 18, even low amounts of ACA in the electrode reduce the strain.

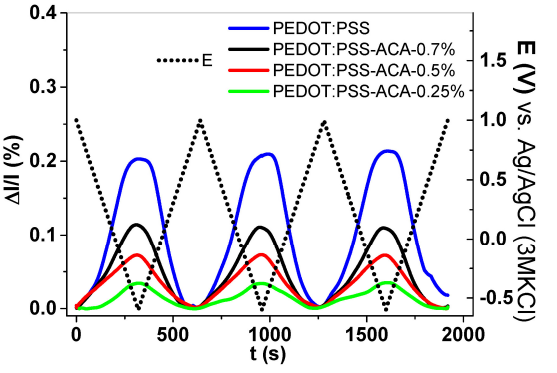

Figure 18. Linear strain of PEDOT:PSS and PEDOT:PSS-ACA (0.7 (black), 0.5 (red) and 0.25% (green)) actuators with PVdF membrane at potential E (+1– –0.65 V) in 0.2 M LiTFSI (in PC) as electrolyte

The highest strain is obtained with the highest concentration of ACA, suggesting that a structural arrangement favorable for ion transport was gradually developed with increase in ACA concentration. The changes in length of PEDOT:PSS-ACA at 4 mN were 0.1% and 0.2% for PEDOT:PSS, suggesting that PEDOT:PSS trilayers are more suitable for applications requiring higher strain and PEDOT:PSS-ACA for applications requiring higher force.

Figure 17 shows that for PEDOT:PSS-ACA actuators at constant potential there is a little drop in stress curve showing a relaxation process. The slopes of the curves upon reduction suggest that PEDOT:PSS-ACA more rapidly becomes saturated by cations. PEDOT:PSS is poorly conductive in the reduced state. Without ACA, the uptake of ions is gradual until the oxidation step. The complex performance of PEDOT:PSS-ACA with both faradaic and non-faradaic charging mechanisms provides a fast reaction when undergoing a potential change, which can be explained by the increased electrical conductivity of the hybrid in both the reduced and oxidised states (Table 3). This is likely due to the porous nature of ACA and enables much faster ion transport – this is also confirmed by diffusion coefficients calculated according to eq 4.

Cyclic voltammogram was recorded in linear actuation mode (Figure 19). There is an oxidation peak at 0.2 V (Figure 19) with a reduction wave at –0.1 V, both related to the uptake of cations as the PSS anions are immobilised in the membrane. On oxidation and reduction, electroneutrality is provided by the cations from the organic electrolyte solvated Li^+ ions.

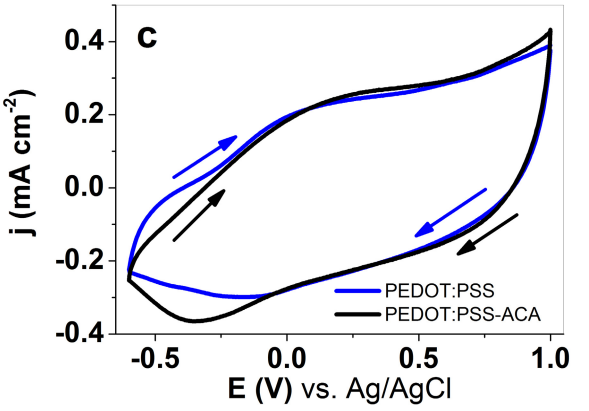

Figure 19. Current density vs applied potential range for PEDOT:PSS and PEDOT:PSS-ACA on PVdF from publication I. 0.2 M LiTFSI in PC electrolyte, scan rate 5 mV s^{-1}

Upon oxidation, the fast contraction of PEDOT:PSS-ACA is followed by a slight increase in the strain. In earlier research, a corresponding decrease in stress on oxidation was observed in carbide-derived-carbon-PPy hybrid actuators [58]. In the case of carbon-based ionic electromechanical actuators, this behavior has been attributed to the two-carrier model, where after cation diffusion out of the material, a small number of anions enter the material, causing expansion [59].

Table 3. Surface conductivity of the PEDOT:PSS and PEDOT:PSS-ACA films in the oxidised and reduced states under N_2 atmosphere

	Electrical conductivity, mS/sq	
	Oxidised (1 V)	*Reduced (−1 V)*
PEDOT:PSS	26 ± 1	4 ± 0
PEDOT:PSS-ACA	60 ± 3	10 ± 0

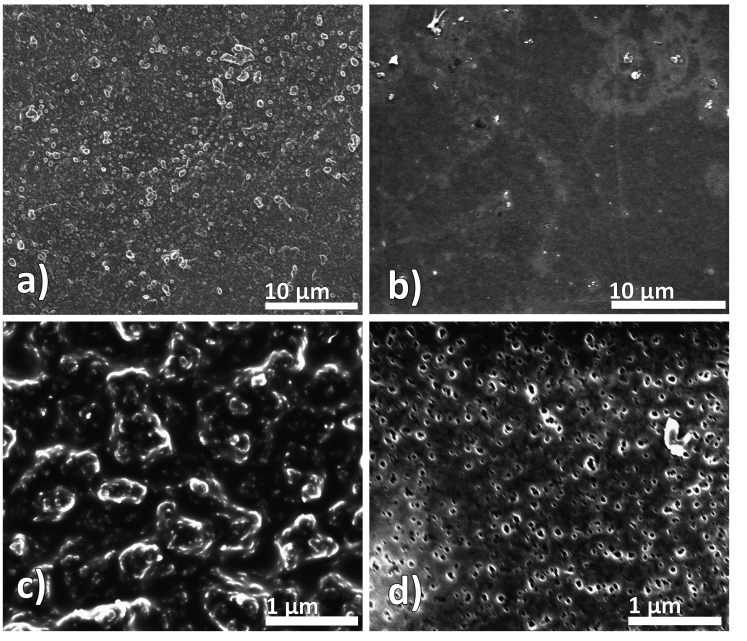

Figure 20. SEM images of topographical representation of the PEDOT:PSS (c, e) and PEDOT:PSS-ACA (d, f) electrodes

The calculated densities of the electrodes based on measured mass and volumes were 1065 ± 2 kg m^{-3} for PEDOT:PSS-ACA electrodes and 1233 ± 34 kg m^{-3} for PEDOT:PSS. Adding carbon to the CP ink makes less dense electrodes. This may be deduced from the SEM image (Figure 20d vs Figure 20c) where added carbon makes the surface much rougher. When growing the thickness of the electrodes via printing, the properties change similarly to PEDOT:PSS electrode actuators – bending strain, force and capacitance growth in the range of 5–20 layers.

E_M is corresponding with the densities of the electrodes: PEDOT:PSS-ACA actuators have lower values than PEDOT:PSS actuators. It also refers to weaker interactions between the PEDOT:PSS matrix and ACA particles.

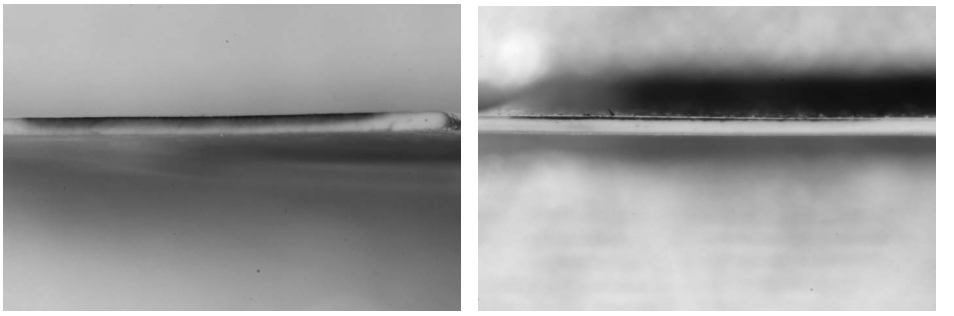

Figure 21. Optical microscopy image, where PEDOT:PSS sinks further into the membrane (left) and PEDOT:PSS-ACA stays on the surface (right). Membrane width 120 µm. Has not been immersed in IL.

The additional effect of carbon in the conducting polymer ink was that it inhibits the ink from submerging too far into the dry PVdF membrane (Figure 21) eliminating the possibility for short circuiting. Therefore, adding ACA to the ink reduces the fabrication time and steps.

Carbide-derived carbon (CDC)-based actuators prepared with casting method have similar frequency dependence with strains up to 0.1–0.6% at 0.002 Hz at 2 V [27], but the printed actuators use much less material (300 µm thick actuator with 100 µm thick electrodes for CDC-based vs 123 µm thick actuators with 4 µm thick electrodes for printed actuators). In addition, compared to CDC-based actuators, the fabrication process takes less time for the printed actuators (a few hours vs. days).

5.4 Miniaturisation

Inkjet-printed electrodes on commercial PVdF gave disproportionate actuators, with membrane being 120 µm and electrodes being 2–10 µm. To get an order of magnitude thinner actuators the commercial PVdF membrane was exchanged for laboratory made spin coated semi interpenetrated NBR/PEO membrane. A high molecular mass elastomer NBR for rigidity in ion conductivity providing PEO network has successfully been demonstrated as a membrane in micro-actuators by [15].

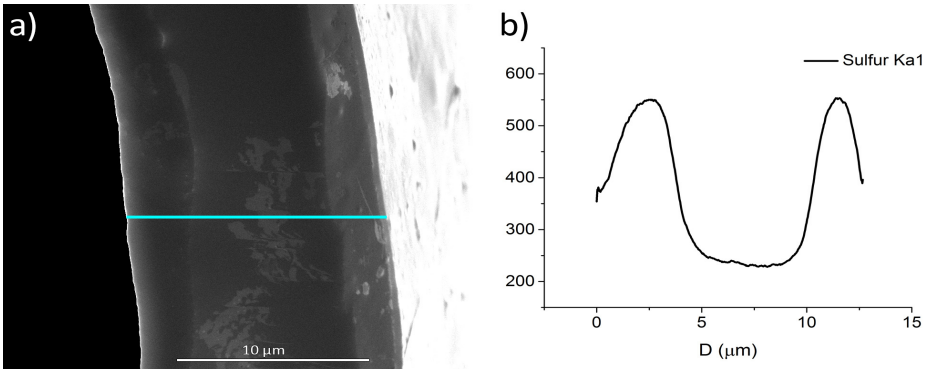

Figure 22. a) SEM image of the cross section of a PEDOT:PSS-semi-IPN trilayer; b) corresponding EDX analysis of sulfur across the cross section

For bending actuation in air an IL [EMIm][TFSI] (Figure 5c) was used as an electrolyte which has previously been applied in IEAPs with NBR/PEO membrane [15,60,61]. PEDOT:PSS-semi-IPN trilayer actuators with 12.7 µm thickness were fabricated (Figure 22).

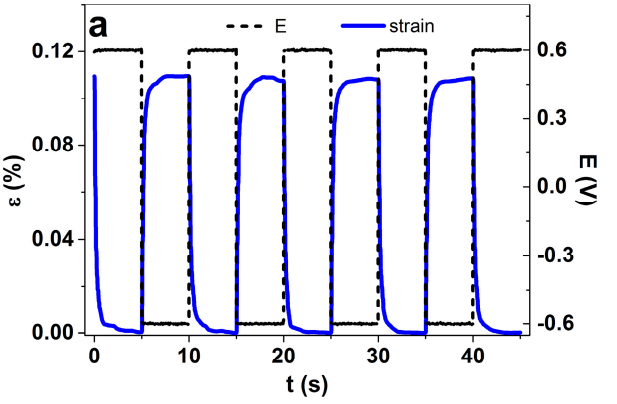

Figure 23. Bending strain for PEDOT:PSS-IPN trilayers with the rectangular actuation voltage ±0.6 V

At 0% strain, a working electrode is oxidised and fully contracted and the maximum strain occurs where the opposite electrode is fully oxidised and fully contracted (Figure 23). The strain is higher at lower frequencies and has a plateau similar to actuators with PEDOT:PSS electrodes on 120 µm membrane. Between 0.005 and 0.3 Hz, the strain decreases only from 0.07% to 0.05% (Figure 26).

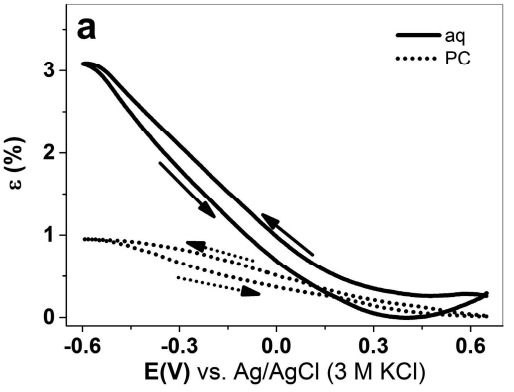

Figure 24. Linear strain for PEDOT:PSS on NBR/PEO membrane network from publication III. 0.2 M LiTFSI in water and in PC electrolytes

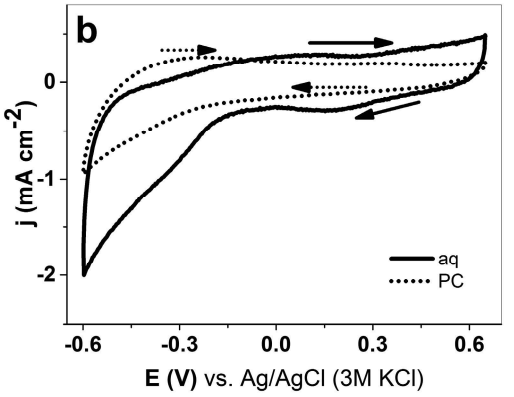

Figure 25. Current density vs applied potential range for PEDOT:PSS on NBR/PEO membrane network from publication III. 0.2 M LiTFSI in water and in PC electrolytes

Contrary to the previous study, where actuation changed direction with changing of the solvent [62], PEDOT:PSS-semi-IPN trilayer shows mainly Li+ driven expansion at reduction, independent of the solvent. For both solvents, the main feature observed is a large wave at negative potentials corresponding to flux of cations [63].

In the case of 10 times thinner NBR/PEO membrane, the current density is 2 times larger in its peak (Figure 25) than for similar actuators with PVdF membrane (Figure 19), making NBR/PEO membrane-based actuators more energy efficient in linear actuation mode. The corresponding linear strain (Figure 24) is also 5 times larger than for actuators with PVdF membrane (Figure 18). The inactive membrane in the actuator is thinner and more elastic (1.1 MPa) [60] than PVdF membrane, thus allowing for larger elongation.

PEDOT:PSS-NBR/PEO in aqueous electrolyte shows significant linear strain – 3%. Bending strain however is smaller at 0.08% at lower frequencies (0.005–1 Hz).

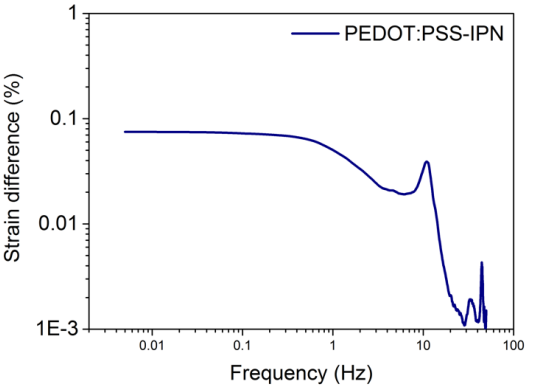

Figure 26. Bending strain difference frequency dependence of PEDOT:PSS on NBR/ PEO interpenetrating networks

First resonance frequency at 11 Hz and second at 44 Hz [15] have shown that microactuators with PEDOT (oxidative polymerisation from EDOT) for electrodes have bending strain difference of 0.6% at 2 V actuation potential and 12 µm thickness at 1 Hz. An actuator with printed electrodes has 0.05% strain at 0.6 V at 1 Hz. In this work, low voltage was used to avert irreversible redox processes.

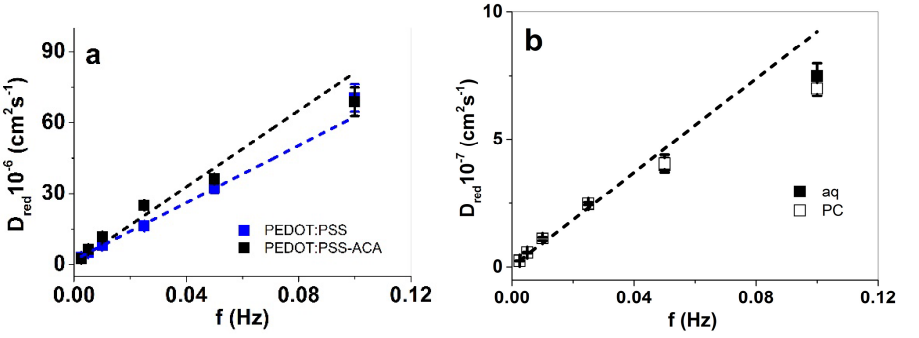

Figure 27. The diffusion coefficients on reduction at different frequencies (a) PEDOT: PSS-(ACA)-PVdF actuators (b) PEDOT:PSS-semi IPN actuators

Figure 27 shows the diffusion coefficients; it can be seen that the diffusion in the PEDOT:PSS-semi IPN actuators is an order of magnitude lower, even though it is much thinner, which can be contributed to a denser membrane with less pores than the PVdF membrane.

Microactuators were fabricated with combined industrial technologies, spin coating and ink-jet printing. These micro PEDOT:PSS-semi-IPN actuators show promising actuation in linear actuation mode. The current work is a good foundation to achieve the industrially applicable fabrication of soft actuators in micro scale using bottom up printing.

6. CONCLUSIONS

Future soft micro actuator applications for biomedical and soft robotic applications need reliable, repeatable, cost-effective and scalable production methods. This work introduced inkjet printing as a promising alternative to other currently known fabrication methods for preparing ionic electromechanical systems. Drop-on-demand printing is a convenient method for fabricating electrodes with intricate and complex patterns without the need for masks. Since ink is deposited only where the pattern design allows, very little electrode material goes to waste, facilitating an environmentally friendly and cost-effective approach. This method that enables the deposition of functional materials in complex patterns, merged with printed electronics, offers the potential for fully printed soft IEAPs with integrated printed electronic systems in the near future.

The electrical, mechanical and actuation properties of printed micro actuators are tunable using various strategies. First, the composition of the ink can be modified to achieve desired results. This work introduced a novel conducting polymer-carbon composite with tunable force and actuation parameters. It was shown that CP-carbon-composite actuators have superior force in linear actuation mode, whereas pure CP actuators have greater strain. Electrochemical studies also confirmed the superior force characteristics of CP-carbon actuators in bending mode, while the strain still remained higher for CP based actuators.

Second, controlling the electrode thickness enables to fine tune actuator properties such as strain, force, conductivity, bending stiffness and capacitance. It was shown that the thickness of printed electrode layers is in very good linear correlation with the number of layers on top of each other (in the range of 5–20 layers). This approach results in highly reproducible actuators with very small standard deviation in the electrode layer thickness. Increasing thickness also increased force, strain and capacitance and sheet conductivity of the electrodes.

Third, the actuator performance can be tailored by the selection of appropriate substrate/membrane materials. Printing on different membrane materials results in composites with different properties. For example, extremely thin (12.7 μm) trilayer actuators were fabricated using spin coated semi-IPN NBR/PEO membranes as substrate for conducting polymer (PEDOT:PSS) electrodes. These novel composites could be actuated both in linear and in bending mode and showed a superior 3% strain in the linear mode, an order of magnitude higher linear strain than that for other tested membrane materials (e.g. commercial PVdF membrane with 0.2% linear strain).

This work has showed that despite the known limitations of the drop-on-demand printing method it is possible to prepare soft electromechanical systems using this technology. With the selection of compatible materials, and by using various strategies to tune the functional properties of the composite towards more preferred outcome it will be possible in the nearest future to realise applications with fully printed and integrated soft electromechanically active components.

7. SUMMARY IN ESTONIAN

Tindiprinditud pehmed aktuaatorid

Ioonsed elektroaktiivsed polümeerid (IEAP) on tihti kolmekihilised materjalid, mis koosnevad kahest ioon- ja elektronjuhtivast elektroodist ja neid eraldavast ioonjuhtivast poorsest membraanist. Looduslikku lihase liigutust meenutav elektrilisele stiimulile vastav liigutus teeb nad atraktiivseks materjaliks mikrosüsteemide jaoks, kus on vaja õrna, vaikset, pikiliigutust või madalat liigutuspinget. Tulevased pehmed täiturid biomeditsiini ja robootika rakenduseteks vajavad usaldusväärset, korratavat ja skaleeritavat valmistamismeetoodikat. See uurimistöö tutvustas tindipritsprintimist kui alternatiivi seni kasutusel olevatele valmistamismeetoditele valmistamaks ioonilisi elektromehaanilisi süsteeme. Piisksadestusprintimine on mugav meetod keeruliste mustritega elektroodide valmistamiseks, ilma et oleks vaja kasutada maske. Kuna tinti sadestatakse ainult sinna, kuhu mustri disain lubab, läheb väga vähe materjali kaotsi, mis teeb sellest keskkonnasõbraliku ja soodsa lähenemise. Selline meetod, mis lubab sadestada funktsionaalseid materjale keeruka mustrina, koos prinditud elektroonikaga pakub juba lähitulevikus võimaluse integreerida täielikult prinditud pehmed IEAP-d prinditud elektroonika süsteemidega.

Prinditud mikrotäiturite elektrilisi, mehaanilisi ja täituromadusi saab erinevatel viisidel häälestada. Esiteks mõjutab täiturite omadusi tindi koostis. Siin töös tutvustati uut juhtivpolümeer-süsinikkomposiiditi, mille jõud ja liigutusulatus on reguleeritavad. Näidati, et juhtivpolümeer-süsinik-komposiidis täituritel on suurem jõud lineaarse liigutuse režiimis (sisuliselt pikenemine-lühenemine), aga puhtal juhtivpolümeer-täituril on suurem liigutusulatus. Elektrokeemilised katsed kinnitasid ka suuremat jõudu juhtivpolümeer-süsinik-täituritel painutusrežiimis ning liigutusulatus jäi kõrgemaks ainult juhtivpolümeeridel põhinevatel täituritel.

Teiseks, saab täituri omadusi (nt liigutusulatus, jõud, juhtivus, painutusjäikus ja mahtuvus) täppisreguleerida elektroodi paksuse varieerimisega. Selles töös näidati, et elektroodi paksus on väga heas lineaarses seoses prinditud kihtide arvuga (5–20 kihi ulatuses). Selline lähenemine võimaldab valmistada hästi korratavate omadustega täitureid. Elektroodide paksuse kasvades kasvas ka täituri jõud, liigutusulatus, mahtuvus ja pinnajuhtivus.

Kolmandaks häälestati täituri sooritust sobivate alus- ehk membraanmaterjalide valikuga. Erinevatele materjalidele printimine annab tulemuseks erinevate omadustega komposiidi. Näiteks väga õhukese (12,7 μm) kolmekihilise täituri valmistamiseks kasutades vurrkatmise abil tehtud (semi-IPN NBR/PEO) membraani, millele prinditi juhtivat polümeeri (PEDOT:PSS). Neid uusi komposiite saab liigutada nii lineaarses kui painutusrežiimis. Nende liigutus lineaarses režiimis oli suurusjärgu võrra suurem kui teisele materjalidele prinditud komposiitidel (3% isevalmistatud membraani korral ja 0.2% tööstusliku PVdF-i korral).

Selles töös näidati, et piisksadestusprintimise teel on võimalik valmistada pehmeid elektromehaanilisi süsteeme, hoolimata meetodi mõningatest piirangutest. Sobivalt valitud tindimaterjalid ja häälestatud printimisprotsess võimaldavad juba lähitulevikus valmistada pehmeid ja integreeritud elektromehaanilisi süsteeme, mis on algusest lõpuni prinditud.

REFERENCES

[1] Baughman, R. H., Shacklette, L. W., Elsenbaumer, R. L., Plichta, E. J. & Becht, C. Micro Electromechanical Actuators Based on Conducting Polymers. in *Molecular Electronics: Materials and Methods* (ed. Lazarev, P. I.) 267–289 (Springer Netherlands, 1991). doi:10.1007/978-94-011-3392-0_27

[2] Alici, G. & Higgins, M. J. Normal stiffness calibration of microfabricated tri-layer conducting polymer actuators. *Smart Mater. Struct.* **18,** 065013 (2009).

[3] Park, J., Jung, S.-H., Kim, Y.-H., Kim, B., Lee, S.-K. & Park, J.-O. Design and fabrication of an integrated cell processor for single embryo cell manipulation. *Lab Chip* **5,** 91 (2005).

[4] Svennersten, K., Berggren, M., Richter-Dahlfors, A. & Jager, E. W. H. Mechanical stimulation of epithelial cells using polypyrrole microactuators. *Lab Chip* **11,** 3287–3293 (2011).

[5] Casadevall i Solvas, X., Lambert, R. A., Kulinsky, L., Rangel, R. H. & Madou, M. J. Micromixing and flow manipulation with polymer microactuators. *Microfluid. Nanofluidics* **11,** 405–416 (2011).

[6] Zhong, Y., Lundemo, S. & Jager, E. W. H. Development of polypyrrole based solid-state on-chip microactuators using photolithography. *Smart Mater. Struct.* **27,** 074006 (2018).

[7] Miller, C., Montgomery, D., Black, M. & Schnetler, H. Thermal expansion as a precision actuator. in *Proc. SPIE 9912, Advances in Optical and Mechanical Technologies for Telescopes and Instrumentation II* (eds. Navarro, R. & Burge, J. H.) 991269 (2016). doi:10.1117/12.2231392

[8] Cugat, O., Delamare, J. & Reyne, G. Magnetic micro-actuators and systems (MAGMAS). *IEEE Trans. Magn.* **39,** 3607–3612 (2003).

[9] Conrad, H., Schenk, H., Kaiser, B., Langa, S., Gaudet, M., Schimmanz, K., Stolz, M. & Lenz, M. A small-gap electrostatic micro-actuator for large deflections. *Nat. Commun.* **6,** 1–7 (2015).

[10] Must, I., Johanson, U., Kaasik, F., Põldsalu, I., Punning, A. & Aabloo, A. Charging a supercapacitor-like laminate with ambient moisture: from a humidity sensor to an energy harvester. *Phys. Chem. Chem. Phys.* **15,** 9605–14 (2013).

[11] Must, I., Kaasik, F., Põldsalu, I., Johanson, U., Punning, A. & Aabloo, A. A carbide-derived carbon laminate used as a mechanoelectrical sensor. *Carbon N. Y.* **50,** 535–541 (2012).

[12] Temmer, R. Electrochemistry and novel applications of chemically synthesized conductive polymer electrodes. (University of Tartu, 2014).

[13] Madden, J. D. W., Vandesteeg, N. A., Anquetil, P. A., Madden, P. G. A., Takshi, A., Pytel, R. Z., Lafontaine, S. R., Wieringa, P. A. & Hunter, I. W. Artificial Muscle Technology: Physical Principles and Naval Prospects. *IEEE J. Ocean. Eng.* **29,** 706–728 (2004).

[14] Hara, S., Zama, T., Takashima, W. & Kaneto, K. Free-standing gel-like polypyrrole actuators doped with bis(perfluoroalkylsulfonyl)imide exhibiting extremely large strain. *Smart Mater. Struct.* **14,** 1501–1510 (2005).

[15] Maziz, A., Plesse, C., Soyer, C., Chevrot, C., Teyssié, D., Cattan, E. & Vidal, F. Demonstrating kHz Frequency Actuation for Conducting Polymer Microactuators. *Adv. Funct. Mater.* n/a-n/a (2014). doi:10.1002/adfm.201400373

[16] Smela, E. Conjugated polymer actuators for biomedical applications. *Adv. Mater.* **15,** 481–494 (2003).

[17] Kim, S.-S., Jeon, J.-H., Kee, C.-D. & Oh, I.-K. Electro-active hybrid actuators based on freeze-dried bacterial cellulose and PEDOT:PSS. *Smart Mater. Struct.* **22,** 085026 (2013).
[18] Punning, A., Vunder, V., Must, I., Johanson, U., Anbarjafari, G. & Aabloo, A. In situ scanning electron microscopy study of strains of ionic electroactive polymer actuators. *J. Intell. Mater. Syst. Struct.* 1045389X15581520- (2015). doi:10.1177/1045389X15581520
[19] Kiefer, R., Aydemir, N., Torop, J., Tamm, T., Temmer, R., Travas-Sejdic, J., Must, I., Kaasik, F. & Aabloo, A. Carbide-derived carbon as active interlayer of polypyrrole tri-layer linear actuator. *Sensors Actuators, B Chem.* **201,** 100–106 (2014).
[20] Lu, W., Fadeev, A. G., Qi, B., Smela, E., Mattes, B. R., Ding, J., Spinks, G. M., Mazurkiewicz, J., Zhou, D., Wallace, G. G., Macfarlane, D. R., Forsyth, S. A. & Forsyth, M. Use of Ionic Liquids for -Conjugated Polymer Electrochemical Devices. *Science* **297,** 983–987 (2002).
[21] Temmer, R., Maziz, A., Plesse, C., Aabloo, A., Vidal, F. & Tamm, T. In search of better electroactive polymer actuator materials: PPy versus PEDOT versus PEDOT–PPy composites. *Smart Mater. Struct.* **22,** 104006 (2013).
[22] Torop, J. *et al.* Carbide-derived Carbon (CDC) linear actuator properties in combination with conducting polymers. *Electroact. Polym. Actuators Devices 2010* **9056,** 76422A (7 pp.) (2014).
[23] Maziz, A., Plesse, C., Soyer, C., Cattan, E. & Vidal, F. Top-down Approach for the Direct Synthesis, Patterning, and Operation of Artificial Micromuscles on Flexible Substrates. *ACS Appl. Mater. Interfaces* **8,** 1559–1564 (2016).
[24] Kiefer, R., Temmer, R., Aydemir, N., Travas-Sejdic, J., Aabloo, A. & Tamm, T. Electrochemistry of interlayer supported polypyrrole tri-layer linear actuators. *Electrochim. Acta* **122,** 322–328 (2014).
[25] Simaite, A., Mesnilgrente, F., Tondu, B., Souères, P. & Bergaud, C. Towards inkjet printable conducting polymer artificial muscles. *Sensors Actuators, B Chem.* **229,** 425–433 (2016).
[26] Ikushima, K., John, S., Ono, A. & Nagamitsu, S. PEDOT/PSS bending actuators for autofocus micro lens applications. *Synth. Met.* **160,** 1877–1883 (2010).
[27] Torop, J., Palmre, V., Arulepp, M., Sugino, T., Asaka, K. & Aabloo, A. Flexible supercapacitor-like actuator with carbide-derived carbon electrodes. *Carbon N. Y.* **49,** 3113–3119 (2011).
[28] Palmre, V., Brandell, D., Mäeorg, U., Torop, J., Volobujeva, O., Punning, A., Johanson, U., Kruusmaa, M. & Aabloo, A. Nanoporous carbon-based electrodes for high strain ionomeric bending actuators. *Smart Mater. Struct.* **18,** 095028 (2009).
[29] Kaasik, F., Must, I., Baranova, I., Põldsalu, I., Lust, E., Johanson, U., Punning, A. & Aabloo, A. Scalable fabrication of ionic and capacitive laminate actuators for soft robotics. *Sensors Actuators B Chem.* **246,** 154–163 (2017).
[30] Chinn, D. & Janata, J. Spin-cast thin films of polyaniline. *Thin Solid Films* **252,** 145–151 (1994).
[31] Põldsalu, I., Mändmaa, S.-E., Peikolainen, A.-L., Kesküla, A. & Aabloo, A. Fabrication of ion-conducting carbon polymer composite electrodes by spin coating. in *Proc. SPIE 9430. Electroactive Polymer Actuators and Devices (EAPAD) 2015* **9430,** 943019 (SPIE, 2015).

[32] Taccola, S., Greco, F., Mazzolai, B., Mattoli, V. & Jager, E. W. H. Thin film free-standing PEDOT:PSS/SU8 bilayer microactuators. *J. Micromechanics Micro-engineering* **23,** 117004 (2013).
[33] Smela, E. Microfabrication of PPy microactuators and other conjugated polymer devices. *J. Micromech. Microeng* **9,** 1–18 (1999).
[34] Vaeth, K. M. & Jensen, K. F. Chemical vapor deposition of thin polymer films used in polymer-based light emitting diodes. *Adv. Mater.* **9,** 490–493 (1997).
[35] Mohammadi, A., Hasan, M.-A., Liedberg, B., Lundström, I. & Salaneck, W. R. Chemical vapour deposition (CVD) of conducting polymers: Polypyrrole. *Synth. Met.* **14,** 189–197 (1986).
[36] Gaihre, B., Alici, G., Spinks, G. M. & Cairney, J. M. Pushing the limits for micro-actuators based on electroactive polymers. *J. Microelectromechanical Syst.* **21,** 574–585 (2012).
[37] Kruusamäe, K., Brunetto, P., Punning, A., Kodu, M., Jaaniso, R., Graziani, S., Fortuna, L. & Aabloo, A. Electromechanical model for a self-sensing ionic polymer–metal composite actuating device with patterned surface electrodes. *Smart Mater. Struct.* **20,** 124001 (2011).
[38] Pede, D., Serra, G. & De Rossi, D. Microfabrication of conducting polymer devices by ink-jet stereolithography. *Mater. Sci. Eng. C* **5,** 289–291 (1998).
[39] Pabst, O., Perelaer, J., Beckert, E., Schubert, U. S., Eberhardt, R. & Tünnermann, A. All inkjet-printed piezoelectric polymer actuators: Characterization and applications for micropumps in lab-on-a-chip systems. *Org. Electron. physics, Mater. Appl.* **14,** 3423–3429 (2013).
[40] Pabst, O., Perelaer, J., Beckert, E., Schubert, U. S., Eberhardt, R. & Tünnermann, A. Inkjet printing of electroactive polymer actuators on polymer substrates. *Proc. SPIE* **7976,** 79762H–79762H–6 (2011).
[41] Hoth, C. N., Schilinsky, P., Choulis, S. A. & Brabec, C. J. Printing Highly Efficient Organic Solar Cells. *Nano Lett.* **8,** 2806–2813 (2008).
[42] Eom, S. H., Senthilarasu, S., Uthirakumar, P., Yoon, S. C., Lim, J., Lee, C., Lim, H. S., Lee, J. & Lee, S. H. Polymer solar cells based on inkjet-printed PEDOT:PSS layer. *Org. Electron. physics, Mater. Appl.* **10,** 536–542 (2009).
[43] Angmo, D., Sweelssen, J., Andriessen, R., Galagan, Y. & Krebs, F. C. Inkjet printing of back electrodes for inverted polymer solar cells. *Adv. Energy Mater.* **3,** 1230–1237 (2013).
[44] Fisslthaler, E., Sax, S., Scherf, U., Mauthner, G., Moderegger, E., Landfester, K. & List, E. J. W. Inkjet printed polymer light-emitting devices fabricated by thermal embedding of semiconducting polymer nanospheres in an inert matrix. *Cit. Appl. Phys. Lett. Appl. Phys. Lett. J. Appl. Phys. Appl. Phys. Lett. Appl. Phys. Lett.* **92,** 183305–519 (2008).
[45] Leppäniemi, J., Aronniemi, M., Mattila, T., Alastalo, A., Allen, M. & Seppä, H. Printed WORM memory on a flexible substrate based on rapid electrical sintering of nanoparticles. *IEEE Trans. Electron Devices* **58,** 151–159 (2011).
[46] Sirringhaus, H., Kawase, T., Friend, R. H., Shimoda, T., Inbasekaran, M., Wu, W. & Woo, E. P. High-Resolution Inkjet Printing of All-Polymer Transistor Circuits. *Science (80–.).* **290,** 2123–2126 (2000).
[47] Yang, L., Rida, A., Vyas, R. & Tentzeris, M. M. RFID tag and RF structures on a paper substrate using inkjet-printing technology. *IEEE Trans. Microw. Theory Tech.* **55,** 2894–2901 (2007).

[48] De Gans, B. J. & Schubert, U. S. Inkjet printing of polymer micro-arrays and libraries: Instrumentation, requirements, and perspectives. *Macromol. Rapid Commun.* **24,** 659–666 (2003).
[49] Weng, B., Shepherd, R. L., Crowley, K., Killard, A. J. & Wallace, G. G. Printing conducting polymers. *Analyst* **135,** 2779 (2010).
[50] Haque, R. I., Vié, R., Germainy, M., Valbin, L., Benaben, P. & Boddaert, X. Inkjet printing of high molecular weight PVDF-TrFE for flexible electronics. *Flex. Print. Electron.* **1,** 015001 (2016).
[51] de Gans, B.-J., Duineveld, P. C. & Schubert, U. S. Inkjet printing of polymers: State of the art and future developments. *Adv. Mater. (Weinheim, Ger.* **16,** 203–213 (2004).
[52] Crispin, X., Jakobsson, F. L. E., Crispin, A., Grim, P. C. M., Andersson, P., Volodin, A., Haesendonck, C. Van, Auweraer, M. Van Der, Salaneck, W. R. & Berggren, M. The Origin of the High Conductivity of Poly(3,4-ethylenedioxythiophene)-Poly(styrenesulfonate) (PEDOT:PSS) Plastic Electrodes. *Chem. Mater.* **18,** 4354–4360 (2006).
[53] Sun, K., Zhang, S., Li, P., Xia, Y., Zhang, X., Du, D., Isikgor, F. H. & Ouyang, J. Review on application of PEDOTs and PEDOT:PSS in energy conversion and storage devices. *J. Mater. Sci. Mater. Electron.* **26,** 4438–4462 (2015).
[54] Microfab Technologies, Inc., Texas, USA. Available at: www.microfab.com.
[55] Kiesewetter, L., Zhang, J. M., Houdeau, D. & Steckenborn, A. Determination of Young Moduli of Micromechanical Thin-Films Using the Resonance Method. *Sensors and Actuators A-Physical* **35,** 153–159 (1992).
[56] Sugino, T., Kiyohara, K., Takeuchi, I., Mukai, K. & Asaka, K. Actuator properties of the complexes composed by carbon nanotube and ionic liquid: The effects of additives. *Sensors Actuators, B Chem.* **141,** 179–186 (2009).
[57] Otero, T. F. & Boyano, I. Comparative Study of Conducting Polymers by the ESCR Model. *J. Phys. Chem. B* **107,** 6730–6738 (2003).
[58] Zondaka, Z., Valner, R., Tamm, T., Aabloo, A. & Kiefer, R. Carbide-derived carbon in polypyrrole changing the elastic modulus with a huge impact on actuation. *RSC Adv.* **6,** 26380–26385 (2016).
[59] Liu, Y., Liu, S., Lin, J., Wang, D., Jain, V., Montazami, R., Heflin, J. R., Li, J., Madsen, L. & Zhang, Q. M. Ion transport and storage of ionic liquids in ionic polymer conductor network composites. *Appl. Phys. Lett.* **96,** (2010).
[60] Festin, N., Maziz, A., Plesse, C., Teyssié, D., Chevrot, C. & Vidal, F. Robust solid polymer electrolyte for conducting IPN actuators. *Smart Mater. Struct.* **22,** 104005 (2013).
[61] Cho, M. S., Seo, H. J., Nam, J. D., Choi, H. R., Koo, J. C., Song, K. G. & Lee, Y. A solid state actuator based on the PEDOT/NBR system. *Sensors Actuators, B Chem.* **119,** 621–624 (2006).
[62] Aydemir, N., Kilmartin, P. A., Travas-Sejdic, J., Kesküla, A., Peikolainen, A. L., Parcell, J., Harjo, M., Aabloo, A. & Kiefer, R. Electrolyte and solvent effects in PPy/DBS linear actuators. *Sensors Actuators, B Chem.* **216,** 24–32 (2015).
[63] Raudsepp, T., Marandi, M., Tamm, T., Sammelselg, V. & Tamm, J. Study of the factors determining the mobility of ions in the polypyrrole films doped with aromatic sulfonate anions. *Electrochim. Acta* **53,** 3828–3835 (2008).

ACKNOWLEDGEMENTS

First, I would like to thank my supervisors Anna-Liisa Peikolainen and Rudolf Kiefer for their support and invaluable guidance during my studies. I appreciate the people in IMS Lab in University of Tartu for making it a friendly and supportive work environment. Special thanks to Pille Rinne, Indrek Must, Urmas Johanson, Tarmo Tamm and Alvo Aabloo.

I would like to acknowledge colleagues in Italy and France – Francesco Greco for kick starting my experiments; Frédéric Vidal, Cédric Plesse, Cédric Vancaeyzeele and Kätlin Rohtlaid for propelling the experiments further.

Finally I would like to thank my family and friends for their continual support and Amiran for being there for me.

PUBLICATIONS

CURRICULUM VITAE

Name: Inga Põldsalu
Date of birth: 29.05.1988
Citizenship: Estonian
E-mail: inga.poldsalu@ut.ee

Education

2012–	University of Tartu, Faculty of Science and Technology, PhD student
2010–2012	University of Tartu, Faculty of Science and Technology, MSc in Technology (Materials Science)
2007–2010	University of Tartu, Faculty of Science and Technology, BSc in Technology (Materials Science)
2001–2007	Tallinn Secondary School in Science

Work experience

2012–2015	University of Tartu, Institute of Technology, Specialist in Materials Technology

Professional self-improvement

2012	Chalmers University of Technology, visiting researcher in Department of Chemical and Biological Engineering
2013, 2014	Istituto Italiano di Tecnologia (IIT), visiting researcher in Center for Micro-BioRobotics IIT@SSSA
2015, 2016	University of Cergy-Pontoise, visiting researcher in Laboratory of Physico-Chemistry of Polymers and Interfaces

Dissertations supervised

Identification of Compatible Substrates for Microprinting of Carbon Aerogel Suspensions, Fred Elhi, BSc in Materials Technology

Publications:

1.1 Scholarly articles indexed by Thompson Reuters Wen of Science:

1. Põldsalu, I., Johanson, U., Tamm, T., Punning, A., Greco, F., Peikolainen, A.-L., Kiefer, R., Aabloo, A. Mechanical and electro-mechanical properties of EAP actuators with inkjet printed electrodes. *Synthetic Metals*, **246,** 122-127 (2018).
2. Põldsalu, I., Rohtlaid, K., Nguyen, T. M. G., Plesse, C., Vidal, F., Khorram, M. S., Peikolainen, A.-L., Tamm, T. & Kiefer, R. Thin ink-jet printed trilayer actuators composed of PEDOT:PSS on interpenetrating polymer networks. *Sensors Actuators B Chem.* **258,** 1072–1079 (2018).

3. Nakshatharan, S. S., Vunder, V., Põldsalu, I., Johanson, U., Punning, A. & Aabloo, A. Modelling and Control of Ionic Electroactive Polymer Actuators under Varying Humidity Conditions. *Actuators* **7,** 7 (2018).
4. Kaasik, F., Must, I., Baranova, I., Põldsalu, I., Lust, E., Johanson, U., Punning, A. & Aabloo, A. Scalable fabrication of ionic and capacitive laminate actuators for soft robotics. *Sensors Actuators B Chem.* **246,** 154–163 (2017).
5. Põldsalu, I., Harjo, M., Tamm, T., Uibu, M., Peikolainen, A.-L. & Kiefer, R. Inkjet-printed hybrid conducting polymer-activated carbon aerogel linear actuators driven in an organic electrolyte. *Sensors Actuators B Chem.* **250,** 44–51 (2017).
6. Must, I., Kaasik, F., Põldsalu, I., Mihkels, L., Johanson, U., Punning, A. & Aabloo, A. Ionic and capacitive artificial muscle for biomimetic soft robotics. *Adv. Eng. Mater.* **17,** 84–94 (2015).
7. Punning, A., Kim, K. J., Palmre, V., Vidal, F., Plesse, C., Festin, N., Maziz, A., Asaka, K., Sugino, T., Alici, G., Spinks, G., Wallace, G., Must, I., Põldsalu, I., Vunder, V., Temmer, R., Kruusamäe, K., Torop, J., Kaasik, F., Rinne, P., Johanson, U., Peikolainen, A.-L., Tamm, T., Aabloo, A. Ionic electroactive polymer artificial muscles in space applications. *Sci. Rep.* **4,** 1–6 (2014).
8. Punning, A., Must, I., Põldsalu, I., Vunder, V., Temmer, R., Kruusamäe, K., Kaasik, F., Torop, J., Rinne, P., Lulla, T., Johanson, U., Tamm, T. & Aabloo, A. Lifetime measurements of ionic electroactive polymer actuators. *J. Intell. Mater. Syst. Struct.* **25,** 2267–2275 (2014).
9. Must, I., Vunder, V., Kaasik, F., Põldsalu, I., Johanson, U., Punning, A. & Aabloo, A. Ionic liquid-based actuators working in air: The effect of ambient humidity. *Sensors Actuators B Chem.* **202,** 114–122 (2014).
10. Vunder, V., Itik, M., Põldsalu, I., Punning, A. & Aabloo, A. Inversion-based control of ionic polymer-metal composite actuators with nanoporous carbon-based electrodes. *Smart Mater. Struct.* **23,** (2014).
11. Must, I., Anton, M., Viidalepp, E., Põldsalu, I., Punning, A. & Aabloo, A. Mechanoelectrical impedance of a carbide-derived carbon-based laminate motion sensor at large bending deflections. *Smart Mater. Struct.* **22,** 104015 (2013).
12. Gözen, I., Shaali, M., Ainla, A., Ortmen, B., Põldsalu, I., Kustanovich, K., Jeffries, G. D. M., Konkoli, Z., Dommersnes, P. & Jesorka, A. Thermal migration of molecular lipid films as a contactless fabrication strategy for lipid nanotube networks. *Lab Chip* (2013).
13. Must, I., Johanson, U., Kaasik, F., Põldsalu, I., Punning, A. & Aabloo, A. Charging a supercapacitor-like laminate with ambient moisture: from a humidity sensor to an energy harvester. *Phys. Chem. Chem. Phys.* **15,** 9605–14 (2013).
14. Gözen, I., Ortmen, B., Põldsalu, I., Dommersnes, P., Orwar, O. & Jesorka, A. Repair of large area pores in supported double bilayers. *Soft Matter* **9,** 2787 (2013).

15. Must, I., Kaasik, F., Põldsalu, I., Johanson, U., Punning, A. & Aabloo, A. A carbide-derived carbon laminate used as a mechanoelectrical sensor. *Carbon N. Y.* **50,** 535–541 (2012).

3.1. Articles in collections indexed by the Thompson Reuters Conference Proceedings Citation Index:

1. Põldsalu, I., Mändmaa, S.-E., Peikolainen, A.-L., Kesküla, A. & Aabloo, A. Fabrication of ion-conducting carbon polymer composite electrodes by spin coating. in *Proc. SPIE 9430, Electroactive Polymer Actuators and Devices (EAPAD)* **9430,** 943019 (2015).
2. Punning, A., Põldsalu, I., Kaasik, F., Vunder, V. & Aabloo, A. Micromechanics of ionic electroactive polymer actuators. in *Proc. SPIE 9430, Electroactive Polymer Actuators and Devices (EAPAD)* 94301K (2015).
3. Punning, A., Must, I., Põldsalu, I., Vunder, V., Kaasik, F., Temmer, R. & Aabloo, A. Long-term degradation of the ionic electroactive polymer actuators. in *Proc. SPIE 9430, Electroactive Polymer Actuators and Devices (EAPAD)* 94300S (2015).
4. Must, I., Kaasik, F., Põldsalu, I., Mihkels, L., Johanson, U., Punning, A. & Aabloo, A. Pulse-width-modulated charging of ionic and capacitive actuators. in *IEEE/ASME International Conference on Advanced Intelligent Mechatronics, AIM* 1446–1451 (2014).
5. Must, I., Johanson, U., Kaasik, F., Põldsalu, I., Punning, A. & Aabloo, A. An ionic liquid-based actuator as a humidity sensor. in *IEEE/ASME International Conference on Advanced Intelligent Mechatronics: Mechatronics for Human Wellbeing, AIM* 1498–1503 (2013).
6. Kaasik, F., Torop, J., Must, I., Soolo, E., Põldsalu, I., Peikolainen, A.-L., Palmre, V. & Aabloo, A. Ionic EAP transducers with amorphous nanoporous carbon electrodes. in *Proc. SPIE 8340, Electroactive Polymer Actuators and Devices (EAPAD)* **8340,** 83400V (2012).
7. Must, I., Kaasik, F., Põldsalu, I., Johanson, U., Punning, A. & Aabloo, A. Carbon-polymer-ionic liquid composite as a motion sensor. in *Proc. SPIE 8340, Electroactive Polymer Actuators and Devices (EAPAD)* 834019 (2012).

ELULOOKIRJELDUS

Nimi: Inga Põldsalu
Sünniaeg: 29.05.1988
Kodakondsus: Eesti
E-mail: inga.poldsalu@ut.ee

Haridustee:

alates 2012	Tartu Ülikool, Loodus- ja Tehnoloogiateaduskond, doktoriõpe
2010–2012	Tartu Ülikool, Loodus- ja Tehnoloogiateaduskond, loodusteaduste magister materjaliteaduses
2007–2010	Tartu Ülikool, Loodus- ja Tehnoloogiateaduskond, loodusteaduste bakalaureus materjaliteaduses
2001–2007	Tallinna Reaalkool

Teenistuskäik:

2012–2015	Tartu Ülikool, Tehnoloogiainstituut, materjalitehnoloogia spetsialist

Ametialane enesetäiendus:

2012	Chalmers University of Technology, külalisteadlane osakonnas Chemical and Biological Engineering
2013, 2014	Istituto Italiano di Tecnologia (IIT), külalisteadlane asutuses Center for Micro-BioRobotics IIT@SSSA
2015, 2016	University of Cergy-Pontoise, külalisteadlane Physico-Chemistry of Polymers and Interfaces laboris

Juhendatud lõputööd:
Süsinikaerogeeli suspensioonide mikroprintimiseks sobivate alsupindade tuvastamine, Fred Elhi, BSc in Materials Technology

Publikatsioonid:
Thompson Reuters Wen of Science andmebaasis kajastatud 1.1 teadusartiklid:

1. Põldsalu, I., Johanson, U., Tamm, T., Punning, A., Greco, F., Peikolainen, A.-L., Kiefer, R., Aabloo, A. Mechanical and electro-mechanical properties of EAP actuators with inkjet printed electrodes. *Synthetic Metals*, **246,** 122-127 (2018).
2. Põldsalu, I., Rohtlaid, K., Nguyen, T. M. G., Plesse, C., Vidal, F., Khorram, M. S., Peikolainen, A.-L., Tamm, T. & Kiefer, R. Thin ink-jet printed trilayer actuators composed of PEDOT:PSS on interpenetrating polymer networks. *Sensors Actuators B Chem.* **258,** 1072–1079 (2018).
3. Nakshatharan, S. S., Vunder, V., Põldsalu, I., Johanson, U., Punning, A. & Aabloo, A. Modelling and Control of Ionic Electroactive Polymer Actuators under Varying Humidity Conditions. *Actuators* **7**, 7 (2018).

4. Kaasik, F., Must, I., Baranova, I., Põldsalu, I., Lust, E., Johanson, U., Punning, A. & Aabloo, A. Scalable fabrication of ionic and capacitive laminate actuators for soft robotics. *Sensors Actuators B Chem.* **246,** 154–163 (2017).
5. Põldsalu, I., Harjo, M., Tamm, T., Uibu, M., Peikolainen, A.-L. & Kiefer, R. Inkjet-printed hybrid conducting polymer-activated carbon aerogel linear actuators driven in an organic electrolyte. *Sensors Actuators B Chem.* **250,** 44–51 (2017).
6. Must, I., Kaasik, F., Põldsalu, I., Mihkels, L., Johanson, U., Punning, A. & Aabloo, A. Ionic and capacitive artificial muscle for biomimetic soft robotics. *Adv. Eng. Mater.* **17,** 84–94 (2015).
7. Punning, A., Kim, K. J., Palmre, V., Vidal, F., Plesse, C., Festin, N., Maziz, A., Asaka, K., Sugino, T., Alici, G., Spinks, G., Wallace, G., Must, I., Põldsalu, I., Vunder, V., Temmer, R., Kruusamäe, K., Torop, J., Kaasik, F., Rinne, P., Johanson, U., Peikolainen, A.-L., Tamm, T., Aabloo, A. Ionic electroactive polymer artificial muscles in space applications. *Sci. Rep.* **4,** 1–6 (2014).
8. Punning, A., Must, I., Põldsalu, I., Vunder, V., Temmer, R., Kruusamäe, K., Kaasik, F., Torop, J., Rinne, P., Lulla, T., Johanson, U., Tamm, T. & Aabloo, A. Lifetime measurements of ionic electroactive polymer actuators. *J. Intell. Mater. Syst. Struct.* **25,** 2267–2275 (2014).
9. Must, I., Vunder, V., Kaasik, F., Põldsalu, I., Johanson, U., Punning, A. & Aabloo, A. Ionic liquid-based actuators working in air: The effect of ambient humidity. *Sensors Actuators B Chem.* **202,** 114–122 (2014).
10. Vunder, V., Itik, M., Põldsalu, I., Punning, A. & Aabloo, A. Inversion-based control of ionic polymer-metal composite actuators with nanoporous carbon-based electrodes. *Smart Mater. Struct.* **23,** (2014).
11. Must, I., Anton, M., Viidalepp, E., Põldsalu, I., Punning, A. & Aabloo, A. Mechanoelectrical impedance of a carbide-derived carbon-based laminate motion sensor at large bending deflections. *Smart Mater. Struct.* **22,** 104015 (2013).
12. Gözen, I., Shaali, M., Ainla, A., Ortmen, B., Põldsalu, I., Kustanovich, K., Jeffries, G. D. M., Konkoli, Z., Dommersnes, P. & Jesorka, A. Thermal migration of molecular lipid films as a contactless fabrication strategy for lipid nanotube networks. *Lab Chip* (2013).
13. Must, I., Johanson, U., Kaasik, F., Põldsalu, I., Punning, A. & Aabloo, A. Charging a supercapacitor-like laminate with ambient moisture: from a humidity sensor to an energy harvester. *Phys. Chem. Chem. Phys.* **15,** 9605–14 (2013).
14. Gözen, I., Ortmen, B., Põldsalu, I., Dommersnes, P., Orwar, O. & Jesorka, A. Repair of large area pores in supported double bilayers. *Soft Matter* **9,** 2787 (2013).
15. Must, I., Kaasik, F., Põldsalu, I., Johanson, U., Punning, A. & Aabloo, A. A carbide-derived carbon laminate used as a mechanoelectrical sensor. *Carbon N. Y.* **50,** 535–541 (2012).

3.1 artiklid Thompson Reuters Conference Proceedings Citation Index poolt refereeritud kogumikus:

1. Põldsalu, I., Mändmaa, S.-E., Peikolainen, A.-L., Kesküla, A. & Aabloo, A. Fabrication of ion-conducting carbon polymer composite electrodes by spin coating. in *Proc. SPIE 9430, Electroactive Polymer Actuators and Devices (EAPAD)* **9430,** 943019 (2015).
2. Punning, A., Põldsalu, I., Kaasik, F., Vunder, V. & Aabloo, A. Micromechanics of ionic electroactive polymer actuators. in *Proc. SPIE 9430, Electroactive Polymer Actuators and Devices (EAPAD)* 94301K (2015).
3. Punning, A., Must, I., Põldsalu, I., Vunder, V., Kaasik, F., Temmer, R. & Aabloo, A. Long-term degradation of the ionic electroactive polymer actuators. in *Proc. SPIE 9430, Electroactive Polymer Actuators and Devices (EAPAD)* 94300S (2015).
4. Must, I., Kaasik, F., Põldsalu, I., Mihkels, L., Johanson, U., Punning, A. & Aabloo, A. Pulse-width-modulated charging of ionic and capacitive actuators. in *IEEE/ASME International Conference on Advanced Intelligent Mechatronics, AIM* 1446–1451 (2014).
5. Must, I., Johanson, U., Kaasik, F., Põldsalu, I., Punning, A. & Aabloo, A. An ionic liquid-based actuator as a humidity sensor. in *IEEE/ASME International Conference on Advanced Intelligent Mechatronics: Mechatronics for Human Wellbeing, AIM* 1498–1503 (2013).
6. Kaasik, F., Torop, J., Must, I., Soolo, E., Põldsalu, I., Peikolainen, A.-L., Palmre, V. & Aabloo, A. Ionic EAP transducers with amorphous nanoporous carbon electrodes. in *Proc. SPIE 8340, Electroactive Polymer Actuators and Devices (EAPAD)* **8340,** 83400V (2012).
7. Must, I., Kaasik, F., Põldsalu, I., Johanson, U., Punning, A. & Aabloo, A. Carbon-polymer-ionic liquid composite as a motion sensor. in *Proc. SPIE 8340, Electroactive Polymer Actuators and Devices (EAPAD)* 834019 (2012).

DISSERTATIONES TECHNOLOGIAE UNIVERSITATIS TARTUENSIS

1. **Imre Mäger**. Characterization of cell-penetrating peptides: Assessment of cellular internalization kinetics, mechanisms and bioactivity. Tartu 2011, 132 p.
2. **Taavi Lehto**. Delivery of nucleic acids by cell-penetrating peptides: application in modulation of gene expression. Tartu 2011, 155 p.
3. **Hannes Luidalepp**. Studies on the antibiotic susceptibility of *Escherichia coli*. Tartu 2012, 111 p.
4. **Vahur Zadin**. Modelling the 3D-microbattery. Tartu 2012, 149 p.
5. **Janno Torop**. Carbide-derived carbon-based electromechanical actuators. Tartu 2012, 113 p.
6. **Julia Suhorutšenko**. Cell-penetrating peptides: cytotoxicity, immunogenicity and application for tumor targeting. Tartu 2012, 139 p.
7. **Viktoryia Shyp**. G nucleotide regulation of translational GTPases and the stringent response factor RelA. Tartu 2012, 105 p.
8. **Mardo Kõivomägi**. Studies on the substrate specificity and multisite phosphorylation mechanisms of cyclin-dependent kinase Cdk1 in *Saccharomyces cerevisiae*. Tartu, 2013, 157 p.
9. **Liis Karo-Astover**. Studies on the Semliki Forest virus replicase protein nsP1. Tartu, 2013, 113 p.
10. **Piret Arukuusk**. NickFects–novel cell-penetrating peptides. Design and uptake mechanism. Tartu, 2013, 124 p.
11. **Piret Villo**. Synthesis of acetogenin analogues. Asymmetric transfer hydrogenation coupled with dynamic kinetic resolution of α-amido-β-keto esters. Tartu, 2013, 151 p.
12. **Villu Kasari**. Bacterial toxin-antitoxin systems: transcriptional cross-activation and characterization of a novel *mqsRA* system. Tartu, 2013, 108 p.
13. **Margus Varjak**. Functional analysis of viral and host components of alphavirus replicase complexes. Tartu, 2013, 151 p.
14. **Liane Viru**. Development and analysis of novel alphavirus-based multifunctional gene therapy and expression systems. Tartu, 2013, 113 p.
15. **Kent Langel**. Cell-penetrating peptide mechanism studies: from peptides to cargo delivery. Tartu, 2014, 115 p.
16. **Rauno Temmer**. Electrochemistry and novel applications of chemically synthesized conductive polymer electrodes. Tartu, 2014, 206 p.
17. **Indrek Must**. Ionic and capacitive electroactive laminates with carbonaceous electrodes as sensors and energy harvesters. Tartu, 2014, 133 p.
18. **Veiko Voolaid**. Aquatic environment: primary reservoir, link, or sink of antibiotic resistance? Tartu, 2014, 79 p.
19. **Kristiina Laanemets**. The role of SLAC1 anion channel and its upstream regulators in stomatal opening and closure of *Arabidopsis thaliana.* Tartu, 2015, 115 p.

20. **Kalle Pärn**. Studies on inducible alphavirus-based antitumour strategy mediated by site-specific delivery with activatable cell-penetrating peptides. Tartu, 2015, 139 p.
21. **Anastasia Selyutina**. When biologist meets chemist: a search for HIV-1 inhibitors. Tartu, 2015, 172 p.
22. **Sirle Saul**. Towards understanding the neurovirulence of Semliki Forest virus. Tartu, 2015, 136 p.
23. **Marit Orav**. Study of the initial amplification of the human papillomavirus genome. Tartu, 2015, 132 p.
24. **Tormi Reinson**. Studies on the Genome Replication of Human Papillomaviruses. Tartu, 2016, 110 p.
25. **Mart Ustav Jr**. Molecular Studies of HPV-18 Genome Segregation and Stable Replication. Tartu, 2016, 152 p.
26. **Margit Mutso**. Different Approaches to Counteracting Hepatitis C Virus and Chikungunya Virus Infections. Tartu, 2016, 184 p.
27. **Jelizaveta Geimanen**. Study of the Papillomavirus Genome Replication and Segregation. Tartu, 2016, 168 p.
28. **Mart Toots**. Novel Means to Target Human Papillomavirus Infection. Tartu, 2016, 173 p.
29. **Kadi-Liis Veiman**. Development of cell-penetrating peptides for gene delivery: from transfection in cell cultures to induction of gene expression *in vivo*. Tartu, 2016, 136 p.
30. **Ly Pärnaste**. How, why, what and where: Mechanisms behind CPP/cargo nanocomplexes. Tartu, 2016, 147 p.
31. **Age Utt**. Role of alphavirus replicase in viral RNA synthesis, virus-induced cytotoxicity and recognition of viral infections in host cells. Tartu, 2016, 183 p.
32. **Veiko Vunder**. Modeling and characterization of back-relaxation of ionic electroactive polymer actuators. Tartu, 2016, 154 p.
33. **Piia Kivipõld**. Studies on the Role of Papillomavirus E2 Proteins in Virus DNA Replication. Tartu, 2016, 118 p.
34. **Liina Jakobson**. The roles of abscisic acid, CO_2, and the cuticle in the regulation of plant transpiration. Tartu, 2017, 162 p.
35. **Helen Isok-Paas**. Viral-host interactions in the life cycle of human papillomaviruses. Tartu, 2017, 158 p.
36. **Hanna Hõrak**. Identification of key regulators of stomatal CO_2 signalling via O_3-sensitivity. Tartu, 2017, 160 p.
37. **Jekaterina Jevtuševskaja**. Application of isothermal amplification methods for detection of *Chlamydia trachomatis* directly from biological samples. Tartu, 2017, 96 p.
38. **Ülar Allas.** Ribosome-targeting antibiotics and mechanisms of antibiotic resistance. Tartu, 2017, 152 p.
39. **Anton Paier.** Ribosome Degradation in Living Bacteria. Tartu, 2017, 108 p.
40. **Vallo Varik.** Stringent Response in Bacterial Growth and Survival. Tartu, 2017, 101 p.

41. **Pavel Kudrin.** In search for the inhibitors of *Escherichia coli* stringent response factor RelA. Tartu, 2017, 138 p.
42. **Liisi Henno.** Study of the human papillomavirus genome replication and oligomer generation. Tartu, 2017, 144 p.
43. **Katrin Krõlov.** Nucleic acid amplification from crude clinical samples exemplified by *Chlamydia trachomatis* detection in urine. Tartu, 2018, 118 p.
44. **Eve Sankovski.** Studies on papillomavirus transcription and regulatory protein E2. Tartu, 2018, 113 p.
45. **Morteza Daneshmand.** Realistic 3D Virtual Fitting Room. Tartu, 2018, 233 p.
46. **Fatemeh Noroozi.** Multimodal Emotion Recognition Based Human-Robot Interaction Enhancement. Tartu, 2018, 113 p.
47. **Krista Freimann.** Design of peptide-based vector for nucleic acid delivery in vivo. Tartu, 2018, 103 p.
48. **Rainis Venta.** Studies on signal processing by multisite phosphorylation pathways of the *S. cerevisiae* cyclin-dependent kinase inhibitor Sic1. Tartu, 2018, 155 p.